Serveur Académique Lausannois SERVAL serval.unil.ch

Author Manuscript

Faculty of Biology and Medicine Publication

This paper has been peer-reviewed but does not include the final publisher proof-corrections or journal pagination.

Published in final edited form as:

Title: Plasma Proteomic Profiles of Cerebrospinal Fluid-Defined Alzheimer's Disease Pathology in Older Adults.

Authors: Dayon L, Wojcik J, Núñez Galindo A, Corthésy J, Cominetti O, Oikonomidi A, Henry H, Migliavacca E, Bowman GL, Popp J

Journal: Journal of Alzheimer's disease : JAD

Year: 2017

Issue: 60

Volume: 4

Pages: 1641-1652

DOI: 10.3233/JAD-170426

In the absence of a copyright statement, users should assume that standard copyright protection applies, unless the article contains an explicit statement to the contrary. In case of doubt, contact the journal publisher to verify the copyright status of an article.

serval
serveur académique lausannois

UNIL | Université de Lausanne
Faculty of Biology and Medicine

Plasma proteomic profiles of CSF-defined Alzheimer pathology in older adults

Loïc Dayon[1, *], Jérôme Wojcik[2], Antonio Núñez Galindo[1], John Corthésy[1], Ornella Cominetti[1], Aikaterini Oikonomidi[3], Hugues Henry[4], Eugenia Migliavacca[1], Gene L. Bowman[1], and Julius Popp[3]

[1]Nestlé Institute of Health Sciences, Lausanne, Switzerland
[2]Quartz Bio, Geneva, Switzerland
[3]CHUV, Old Age Psychiatry, Department of Psychiatry, Lausanne, Switzerland
[4]CHUV, Department of Laboratories, Lausanne, Switzerland

Running title: Plasma Protein Predictors of Alzheimer

Email: loic.dayon@rd.nestle.com ; jerome.wojcik@quartz.bio; antonio.nunezgalindo@rd.nestle.com; john.corthesy@rd.nestle.com; ornella.cominetti@rd.nestle.com; oikonomidi@yahoo.com; hugues.henry@chuv.ch; eugenia.migliavacca@rd.nestle.com; gene.bowman@rd.nestle.com; julius.popp@chuv.ch

Correspondence to: *Nestlé Institute of Health Sciences, EPFL Innovation Park, Bâtiment H, 1015 Lausanne, Switzerland; Email: loic.dayon@rd.nestle.com, Phone: +41 21 632 6114, Fax: +41 21 632 6499

Abstract

Background: Cerebrospinal fluid (CSF) biomarkers of the beta-amyloid and microtubule associated protein tau metabolism have proven the capacity to improve classification of subjects developing Alzheimer disease (AD). The blood plasma proteome was characterized to further elaborate upon the mechanisms involved and identify proteins that may improve classification of older adults developing an AD dementia.

Objective: Identify and describe plasma protein expressions that best classify subjects with CSF-defined presence of AD pathology and cerebral amyloidosis.

Methods: We performed a cross-sectional analysis of samples collected from community-dwelling elderly with (n = 72) or without (n = 48) cognitive impairment. CSF Aβ1-42, tau and phosphorylated tau (P-tau181) were measured using ELISA and mass spectrometry quantified the plasma proteomes. Presence of AD pathology was defined as CSF P-tau181/Aβ1-42 > 0.0779 and presence of amyloidosis was defined as CSF Aβ1-42 < 724 pg/mL.

Results: Two hundred and forty-eight plasma proteins were quantified. Plasma proteins did not improve classification of the AD CSF biomarker profile in the whole sample. When the analysis was separately performed in the cognitively impaired individuals, the diagnosis accuracy of AD CSF profile was 88.9% with 19 plasma proteins included. Within the full cohort, there were 16 plasma proteins that improved diagnostic accuracy of cerebral amyloidosis to 92.4%.

Conclusion: Plasma proteins improved classification accuracy of AD pathology in cognitively-impaired older adults and appeared representative of amyloid pathology. If confirmed, those candidates could serve as valuable blood biomarkers of the preclinical stages of AD or risk of developing AD.

Keywords

Alzheimer's disease; Amyloid beta; Aβ; Amyloidosis; Biomarker; Dementia; Protein; Tau

Introduction

The prevalence of dementia is expanding rapidly and Alzheimer disease (AD) represents its most common form (60-80% of cases) [1]. AD is characterized by a long prodromal phase that precedes the apparition of the symptoms, with accumulation of amyloid-beta (Aβ) plaques and aggregation of hyperphosphorylated tau as neurofibrillary tangles in the brain [2]. This long prodromal stage poses several challenges to define accurate and early enough AD diagnostics for tailoring and monitoring intervention strategies [3, 4].

The quest for blood-based biomarkers for neurological disorders is pursued by many researchers due to the easily available, minimally invasive and repeatable sampling of blood. Research in the AD field has generated several candidates but well-accepted molecular biomarkers are still measured in cerebrospinal fluid (CSF) [5]. In particular, protein biomarkers in plasma or serum have been reported to differentiate AD or mild-cognitive impairment (MCI) from non-demented controls [6]. Unfortunately, most of the discovery findings have not been replicated, preventing the translation into an AD diagnostic test of clinical utility. This lack of replication might be due to several causes, either inherent to the technology or the biology, but also characteristic of the difficulty of designing proper case-control studies for a disease with such a long prodromal stage. To address such a challenge, endophenotype approaches have been followed [7], where pathology profiles of AD are used as proxy measures. According to the temporal model of AD biomarker alterations by Jack *et al.* [8], decreased concentration of CSF Aβ1-42 constitutes the earliest detectable event and may precede the onset of dementia by more than 20 years [9]. It is

followed by increased concentration of CSF tau, brain atrophy, and impairment in brain glucose metabolism. Blood-based biomarkers that can reflect CSF Aβ1-42 and tau concentrations are therefore of particular interest. As amyloid pathology develops at very early disease stages, CSF Aβ1-42 may be considered as an early pre-dementia and pre-clinical stage biomarker of AD [7].

In this study, we applied a state-of-the-art mass spectrometry (MS)-based proteomics workflow [10] to measure plasma proteome profiles of 120 older community-dwelling adults. While many MS-based proteomic biomarker discovery studies have been performed in cohorts of very limited size due to technical limitations, our highly automated methodology can analyze hundreds of samples and provide sufficient statistical power to deliver robust discovery findings [11]. Using an endophenotype approach to define preclinical AD and cerebral amyloidosis based on CSF measurements of phosphorylated tau 181 (P-tau181)/Aβ1-42 ratio and Aβ1-42 concentration respectively, we aimed at identifying plasma-based protein biomarker candidates that could detect positive CSF profiles of AD pathology and amyloidosis to provide mechanistic insights and potential diagnostics sensitive to the preclinical stages of AD.

Materials and methods

Study population. One hundred and twenty community dwelling participants were included in this study, of whom 48 were cognitively healthy volunteers and 72 had mild cognitive impairment (mild cognitive impairment (MCI), $n = 63$, or mild dementia of AD type, $n = 9$) [12]. Diagnosis of mild cognitive MCI or dementia was based on neuropsychological and clinical evaluation, and made by a consensus conference of psychiatrists and/or neurologists, and neuropsychologists prior to the inclusion into the study. The participants with cognitive

impairment were recruited among outpatients who were referred to the Memory Clinics, Departments of Psychiatry, and Department of Clinical Neurosciences, University Hospitals of Lausanne (Switzerland). They had no major psychiatric disorders, nor substance abuse or severe or unstable physical illness that may contribute to cognitive impairment, had a clinical dementia rating (CDR) [13] score > 0, and met the clinical diagnostic criteria for MCI [14] or AD mild dementia according to the recommendations from the National Institute on Aging and Alzheimer's Association [15]. In the current study, 9 subjects met criteria for probable AD dementia. As there is a clinical continuum between MCI and mild dementia, and the participants with cognitive impairment were patients from memory clinics recruited in the same way irrespective of MCI or mild dementia classification, these subjects were collapsed and labeled as cognitively impaired with CDR > 0. The control subjects were recruited through journal announcements or word of mouth and had no history, symptoms, or signs of relevant psychiatric or neurologic disease and no cognitive impairment (CDR = 0). All participants underwent a comprehensive clinical and neuropsychological evaluation, structural brain imaging, and venous and lumbar punctures [12]. Magnetic resonance imaging and computerized tomography scans were used to exclude cerebral pathologies possibly interfering with the cognitive performance.

Neuropsychological tests were used to assess cognitive performance in the domains of memory [16], language, and visuo-constructive functions. The mini mental state examination [17] was used to assess participants' global cognitive performance. Depression and anxiety were assessed using the hospital anxiety and depression scale [18]. The psychosocial and functional assessments included the activities of daily living (ADL) and instrumental ADL, the neuropsychiatric inventory questionnaire and informant questionnaire on cognitive decline in the elderly [19], and were completed by the family members of the participants. All tests and scales are validated and widely used in the field.

The institutional ethical committee from the University Hospitals of Lausanne approved the clinical protocol (No. 171/2013) and all participants or their legally-authorized representatives signed written informed consent.

CSF and *plasma sample collection.* Venous and lumbar punctures were performed between 8:30-9:30 am after overnight fasting. For lumbar puncture, a standardized technique with a 22 gauge "atraumatic" spinal needle and a sitting or lying position was applied [20]. A volume of 10-12 mL of CSF was collected in polypropylene tubes. Routine cell count and protein quantification were performed. Remaining CSF was frozen in aliquots (500 µL) no later than 1 h after collection and stored at -80 °C without thawing until assay. Blood was drawn into EDTA K3 containing S-Monovette (Sarstedt, Nümbrecht, Germany). After maximum 20-30 min on ice, the tubes were centrifuged at 3000 rpm for 12 min at 6 °C. Volumes of 350 µL plasma samples were aliquoted 2-5 min after centrifugation into polypropylene tubes, frozen no later than 1 h after collection, and stored at -80 °C. Plasma aliquots were not thawed before the proteomic experiment.

CSF Aβ1-42, tau, P-tau181 and APOE ε4 genotyping. The measurements were performed using commercially available ELISA kits and Taqman assays as described in **Supplementary Methods** of the **Supplementary Material**. CSF and blood samples were collected as previously described [12].

Primary outcome measures - CSF profile of AD pathology (AD CSF profile). A pathological AD CSF profile was defined as CSF P-tau181/Aβ1-42 ratio > 0.0779 (*i.e.*, "high" ratio for positive CSF profiles of AD pathology), based on clinical study site data [21] and in line with previous works (*i.e.*, 0.08) [22]. The cutoff optimized the Youden index [23] of the receiver operating characteristic (ROC) curve for the prediction of CDR categories (CDR = 0 *versus* CDR

> 0) (**Supplementary Figure S1A**) as previously reported [12], where the cutoff for CSF P-tau181/Aβ1-42 ratio was further confirmed to be a highly significant predictor of cognitive decline.

Primary outcome measures - CSF profile of amyloid pathology (amyloid pathology CSF profile). Subjects were classified into two groups on the basis of their CSF Aβ1-42 concentrations as "low" when [Aβ1-42] < 724 pg/mL or "high" when [Aβ1-42] ≥ 724 pg/mL, considered as positive and negative CSF profiles of amyloid pathology, respectively. The cutoff optimized the Youden index [23] of the ROC curve for the prediction of CDR categories (CDR = 0 *versus* CDR > 0) (**Supplementary Figure S1B**).

Proteomic analysis. Plasma samples were measured using a shotgun proteomic workflow based on liquid chromatography (LC) tandem MS (MS/MS), as previously reported [10] and described in details in the **Supplementary Methods** of the **Supplementary Material**. Relative quantification of proteins between the samples was obtained using isobaric tagging with the tandem mass tag (TMT) technology [24].

Biomarker quality control. In total, 422 human proteins were identified in the plasma samples. Proteins with greater than 5% missingness were excluded, leaving 248 quality-controlled proteins (**Supplementary Table TS1**). Remaining missing data (5% or less per protein) were imputed by randomly drawing a value between the observed range of biomarker values. Log2 of the protein ratio fold changes were scaled to mean 0 and standard deviation of 1 prior to statistical analyses. Two samples were removed because of aberrant values of the internal standard (**Supplementary Methods** of the **Supplementary Material**), leaving plasma proteomic data available for 118 subjects.

A strong clustering effect was observed in the heatmap of the plasma proteome profiles (**Supplementary Figure S2**). This effect involved 37 proteins with clear differential abundance pattern. It was not associated with any of the available clinical covariates but with other molecular measures in plasma such as amino-acids and microRNAs (data not shown). Those 37 proteins were carried further for the statistical analysis but are marked with # when mentioned in the text.

Statistical analyses. Calculation and statistics were performed with R version 3.3.2 (http://www.r-project.org/). Least absolute shrinkage and selection operator (LASSO) logistic regression [25] selected biomarkers that best predict CSF profiles of AD and amyloid pathology. A reference model was initially generated, testing variables that are likely to be available to clinicians and known risk factors for AD to provide a benchmark for comparison with the models that included plasma proteins. These inputs included age, gender, years of education, and presence of the APOE ε4 allele. In addition of all variables used to make the reference models, protein measurements and CSF albumin index were then included in building so-called best models. A 10-fold cross-validation process was performed for each LASSO analysis using the glmnet package [26], which allows estimating the confidence interval of the misclassification error for each value of the regularization parameter λ. The LASSO analyses were repeated 100 times (1000 times for the reference models). The models that minimized the upper limit of the cross-validated misclassification error confidence interval across the 100 runs with less than 20 features were selected. Their performance was assessed by ROC area under the curve (AUC) estimation using a bootstrap approach with 1000 iterations [27]. Results were compared visually and formally tested for significance against the reference model using ROC AUC [28] and accuracy using a McNemar test.

The group differences for the proteins selected in the best models were graphically illustrated in boxplots and assessed using *t*-test statistics, adjusted for multiple testing by the total number of proteins tested with Bonferroni correction.

Results

Demographic and clinical characteristics of the study population. Demographics and clinical characteristics of the patient cohort are detailed in **Table 1**. The cognitively impaired subjects with MCI and mild dementia were considered together as one group (CDR > 0) (see the **Materials and methods** section); they were older and less educated, with higher prevalence of APOE ε4 genotype compared with the cognitively intact group (CDR = 0). In cognitive impairment, CSF Aβ1-42 was lower while CSF tau, CSF P-tau181, CSF P-tau181/Aβ1-42 and CSF albumin index were all higher.

The classification analysis of the CSF P-tau181/Aβ1-42 ratios aimed first at separating 42 patients with high-expression CSF profile (P-tau181/Aβ1-42 > 0.0779) from 78 low-expression profile subjects in the complete analysis set (**Table 1**), irrespectively of the clinical diagnosis. Then the analysis was performed on the subset of cognitively impaired patients. In this subpopulation, 41 and 31subjects had high and low-expression of AD CSF biomarker profile, respectively.

The classification analysis of the CSF Aβ1-42 concentration categories aimed at separating 47 patients with low-expression CSF profile ([Aβ1-42] < 724 pg/mL) from 73 high-expression profile subjects (**Table 1**), irrespectively of the clinical diagnosis.

Reference benchmark for the prediction of AD CSF profile. In the whole sample, the selected reference model for classification of CSF P-tau181/Aβ1-42 included age and presence of the APOE ε4 allele. Its prediction accuracy was 78.3% (as compared to the accuracy of a majority class prediction [29] of 64.4%) and its AUC under the ROC curve was 0.83 (95% confidence interval [0.74-0.90]) (**Figure 1A** and **Table 2**).

In the subset of cognitively impaired subjects, the reference model to classify AD CSF biomarker profile included age, gender, years of education, and presence of APOE ε4 allele, with a prediction accuracy of 77.8% (majority class prediction of 56.9%) and an AUC under the ROC curve of 0.83 [0.73-0.91] (**Figure 1B** and **Table 2**).

Plasma proteins and prediction of AD CSF profile. Protein biomarkers were not able to improve the prediction of AD CSF biomarker profile with respect to the reference model (**Figure 1A**, **Table 2**, and **Supplementary Figure S3A**). The best model accuracy was 80.5% (McNemar *p*-value of 0.1814 when compared with reference model) and AUC under the ROC curve was 0.88 [0.81-0.93] (p = 0.1414 *versus* the reference model as shown in **Figure 1A**). It included four proteins (**Supplementary Table TS1**) in addition of age and presence of APOE ε4 allele. Despite not leading to a significant improvement, all four proteins displayed significant group comparison differences, *i.e.*, insulin-like growth factor-binding protein 2 (IBP2) ($p = 9.3 \times 10^{-5}$), complement component C7 (CO7) ($p = 4.9 \times 10^{-4}$), noelin (NOE1) ($p = 1.3 \times 10^{-3}$), and apolipoprotein E (APOE) (p = 0.04) (**Supplementary Figure S4**).

When considering separately the cognitively impaired subjects, inclusion of protein biomarkers improved significantly diagnostic accuracy to 88.9% (McNemar *p*-value of 0.0990) with an AUC under the ROC curve of 0.96 [0.90-0.99] (p = 0.0038 as shown in **Figure 1B**; see also **Table 2** and **Supplementary Figure S3B**). In total, 19 proteins (**Supplementary Table TS1**) were included in this best model in addition of presence of APOE ε4 allele. Among those proteins,

seven displayed significant difference between the groups: IBP2 ($p = 3.0 \times 10^{-3}$), CO7 ($p = 0.01$), apolipoprotein M (APOM) ($p = 0.02$), selenoprotein P (SEPP1) ($p = 0.02$), NOE1 ($p = 0.04$), angiotensinogen (ANGT) ($p = 0.04$), and pregnancy zone protein (PZP) ($p = 0.05$) (**Supplementary Figure S5**).

Reference benchmark for the prediction of amyloid pathology CSF profile. The reference model for classification of CSF Aβ1-42 was composed of age, gender, years of education, and presence of the APOE ε4 allele. Its prediction accuracy was 80.0% (as compared to the accuracy of a majority class prediction of 60.2%) and its AUC under the ROC curve was 0.86 [0.78-0.92] (**Figure 2A** and **Table 2**).

Plasma proteins and prediction of amyloid pathology CSF profile. Plasma protein biomarkers were able to predict CSF Aβ1-42 categories with high accuracy, *i.e.*, diagnostic accuracy of 92.4% (McNemar *p*-value of 0.0022) and AUC under the ROC curve of 0.96 [0.93-0.99] ($p = 0.0040$ as shown in **Figure 2A**; see also **Table 2**, and **Supplementary Figure S6**). In total 16 proteins (**Supplementary Table TS1**) were selected in this best model in addition of age and presence of APOE ε4 allele. As shown in **Figure 2B**, significant group differences were observed for IBP2 ($p = 2.4 \times 10^{-3}$), uncharacterized protein KIAA0753 (K0753) ($p = 3.2 \times 10^{-3}$), CO7 ($p = 9.5 \times 10^{-3}$), C-reactive protein (CRP) ($p = 0.01$), ovochymase-1 (OVCH1) ($p = 0.01$), ceruloplasmin (CERU) ($p = 0.02$), and sex hormone-binding globulin (SHBG) ($p = 0.02$).

Protein panel overlaps and annotations. In total, 32 plasma proteins were included in all three best models presented above for classification of CSF-defined AD and amyloid pathology. The overlap of the molecular protein panels for classification of AD CSF profile in the whole sample and the subset with cognitive impairment is illustrated with the Venn Diagram of **Figure 3A**, showing IBP2, CO7, and NOE1 proteins as commonly selected features. The protein overlap between biomarker panels improving the classification of AD and brain amyloidosis CSF profiles

appears on **Figure 3B**. Again, IBP2 and CO7 were present in both classification models. Plasma IBP2 and CO7 presented higher abundance in AD and amyloid pathology CSF profiles (**Supplementary Figure S4** and **Figure 1B,** respectively).

Based on the tissue-based map of the human proteome [30], only NOE1 was found to be reported as enriched in the cerebral cortex among the 32 proteins reported in this study. We measured increased levels of plasma NOE1 in individuals with AD CSF biomarker profile (**Supplementary Figures S4** and **S5)**.

Discussion

In the present study, plasma proteome profiles of 120 elderly subjects were measured with MS-based proteomics using a highly automated shotgun workflow [31]. We evaluated if proteins in the peripheral circulation do accurately reflect the presence of cerebral AD pathology or cerebral amyloidosis as measured using well-established CSF biomarkers, and developed diagnostic classification models, so-called best models, to outperform benchmark reference models including variables likely available to clinicians and known risk factors for AD. We found 2 panels of plasma proteins improving the diagnostic accuracy of CSF-defined AD pathology and amyloidosis. Age and presence of APOE ε4 allele were variables relevant to most of the diagnostic classification models.

In our study, plasma proteins were useful to diagnose AD CSF profile defined as higher CSF P-tau181/Aβ1-42 ratios (*i.e.*, > 0.0779) only in the subset of cognitively impaired subjects. This restricted finding is likely due to the low number of subjects with an AD CSF profile in the group of subjects with normal cognition and do not exclude AD specific plasma protein alterations in

the asymptomatic disease stages. As CSF Aβ1-42 is considered as one of the earliest biomarkers of the preclinical development of cerebral AD pathology, we further investigated if plasma proteins could be used to classify CSF Aβ1-42 categories for early stage identification of susceptibility for AD. In our study, 16 proteins were selected for diagnostic classification of amyloid pathology. IBP2, K0753, CO7, CRP, OVCH1, CERU, and SHBG were significantly different between amyloidosis and non-amyloidosis representative CSF profiles.

Plasma and serum protein panels have been proposed as biomarkers of AD pathology by several groups. Most significant findings have been previously [6, 7, 18] and recently [32] reviewed. Ray et *al.* reported an 18-protein panel to classify AD *versus* control subjects with a diagnostic accuracy of 90% [20]. Serum protein-based biomarkers were combined with clinical information (*i.e.*, age, gender, education, and APOE status) to classify AD from controls with 94% sensitivity and 84% specificity while 84% sensitivity and 78% specificity were obtained using clinical variables alone [16]. Another example is the study by Doecke *et al*., reporting an 18-biomarker signature panel on top of age, gender and APOE ε4 genotype for the diagnosis of AD with sensitivity and specificity of 85% with respect to the 77% achieved with only the demographic variables. A panel of 10 proteins predicting progression to AD with 87% accuracy was described by Hye *et al.* [19]. In our study, diagnostic accuracy improvement from 77.8% to 88.9% (+ 14.3%) following the inclusion of plasma protein biomarkers for the classification of AD CSF profile in cognitive impairment appears therefore pertinent. This accuracy improvement may be particularly helpful in memory clinic patients with cognitive impairment to identify those at high risk of having cerebral AD pathology. As blood-based diagnostic methods are non-invasive and easily available, they may be largely used to select patients for additional investigation with more invasive and/or expensive tools such as diagnostic lumbar puncture and positron emission tomography (PET). In addition, identifying subjects likely to have cerebral amyloid pathology

may be particularly important for the recruitment in prevention trials as well as for disease-modifying therapeutic interventions targeting amyloid and starting at preclinical or very early clinical disease stages. In this view, the diagnostic accuracy improvement for the classification of amyloid pathology CSF profile from 80.0% to 92.4% (+ 15.5%) using plasma proteins offers interesting perspectives.

Taken together, our results highlighted the strong contribution of three plasma proteins (*i.e.*, IBP2, CO7, and NOE1) for better classification of CSF pathological profiles (**Figure 3**). In the brain, IBP2 is produced by astroglia and choroid plexus epithelial cells. , It is in the brain the most abundant of the six insulin-like growth factor-binding proteins, whose role is to regulate the availability and activity of insulin-like growth factors [33]. In previous works, IBP2 concentration in the CSF was found to be 20% of that in the circulation [34] but both levels were increased in AD [35]. In line with our results, IBP2 was part of a blood-based signature to determine AD [36] and increased circulating plasma levels were associated with brain atrophy [37]. Plasma IBP2 has also been shown to be related to neurodegeneration, particularly among amyloid negative individuals, suggesting its role in non-AD neurotrophic signaling pathway [38]. In our study, IBP2 contributed to classify both positive CSF profiles of AD pathology and amyloidosis. Complement proteins are present in amyloid plaques and cerebral vascular amyloid in Alzheimer brains; they are observed at the earliest stages of amyloid deposition and their activation corresponds with AD clinical expression [39]. Therefore, the complement system may be an attractive target for therapeutic intervention [40, 41]. We reported plasma CO7, one of the five complement proteins of the membrane attack complex which participate to the late events of complement activation, to be elevated in the pathology status reflected by both abnormal CSF P-tau181/Aβ1-42 and Aβ1-42. To the best of our knowledge, our findings on plasma NOE1 are novel. NOE1 is a secreted glycoprotein expressed in neurogenic tissues during development, and

has an important role in regulating the production of neural crest cells [42]. As a brain-specific protein, NOE1 significant up-regulation in the plasma of subjects with positive CSF biomarker profile of AD might offer compelling diagnostic perspectives.

Several proteins included in our putative classification models have previously been reported. The ε4 allele of APOE is a well-known and major genetic risk factor for AD. In addition, decreased plasma APOE protein levels have been shown in AD [36, 43], in accordance to our results. Furthermore, low plasma APOE has been found to be associated with increased risk of AD and dementia [44]. On the contrary, using a proteomic approach, plasma APOE concentration was found indicative of brain amyloid burden and a positive correlation was evidenced [45]. An additional apolipoprotein reported in our study is APOM which is mainly associated with high-density lipoprotein in plasma [46]. APOM gene was excluded as genetic determinant of AD [47]. But recently, APOM in CSF was found decreased in AD cases [48]. We reported herein increased plasma levels of APOM in subjects with AD CSF profile.

SEPP1 has also been previously associated with Alzheimer pathology [49], underlining the implication of selenium and its antioxidant properties; increased levels of SEPP1, as seen here in AD, might be a response to oxidative stress. SEPP1 protects neuronal cells from Aβ-induced toxicity, suggesting a neuroprotective role of SEPP1 in preventing neurodegenerative disorders [50]. There are contradictory findings about CERU level changes in the blood of AD patients. No difference was observed when comparing its concentration in plasma or serum of AD patients to that of controls [51, 52]. In the plasma of patients with aberrant CSF levels of Aβ1-42, tau and its phosphorylated form, CERU was found to be decreased compared with AD patients with normal levels of these biomarkers in the CSF [53]. But serum copper and CERU levels were found significantly higher in AD than control group [54]. In our study, we detected using shotgun

proteomics higher plasma CERU levels in individuals with the pathological CSF Aβ1-42 profile when compared to those of controls.

An activation of inflammatory pathways is observed in AD [55]. CRP is generally released by the body in response to acute injury, infection, or other inflammatory stimuli. Nonetheless, reduced levels of plasma and serum CRP have been observed in AD [56-59], in agreement with results on the present cohort previously obtained using immunoassays [12]. Herein, we additionally highlighted that decreased plasma level of CRP agreed with amyloid pathology CSF profile.

PZP (a close homolog of the antiprotease alpha-2-macroglobulin and one of the major pregnancy-associated plasma proteins) and SHBG (a glycoprotein that binds androgen and estrogen hormones) are known to be present at different levels in females when compared to males [11]. PZP was found elevated in the serum of women in presymptomatic AD compared with controls [60]. Our results showed somehow the opposite, with decreased plasma levels in AD CSF profile. Muller *et al.* have observed that in both men and women higher levels of SHBG were associated with an increased risk for AD and overall dementia [61]. Patients with AD had higher plasma levels of SHBG [62]. Furthermore, we detected with proteomics an increase of plasma SHBG in individuals with amyloid pathology CSF profile.

ANGT is a component of the renin-angiotensin system, a hormone system that regulates blood pressure and fluid balance. Up-regulation of the renin-angiotensin system in AD brains was reported and our observation of increased ANGT in the plasma of patients with AD CSF profile appeared therefore consistent [63]. To our knowledge, neither K0753 protein, which was recently reviewed as protein moonraker (MOONR), nor OVCH1, have been linked before to AD or neurodegeneration.

In conclusion, our proteomic results suggest that several panels of plasma proteins are relevant to CSF-defined AD and amyloid pathology. The plasma proteome profiles have been obtained on

120 individuals using MS to guarantee more robust findings at the discovery phase than usually performed with such MS-based proteomic approaches. The cohort size remains however limited. Another limitation lies in the two different methods for recruitment of cognitively impaired subject and healthy controls that might induce cohort effect. But, the identified plasma proteins may serve to improve differential diagnosis in cognitively impaired older adults and to facilitate identification of subjects at risk of developing AD that could benefit from prevention strategies or clinical trials focusing on amyloid pathology. As a blood test would be less invasive and expensive than lumbar puncture and PET scans, the results are therefore encouraging but replication in an independent cohort will be needed as well as the results confirmed in relation to longitudinal change before further translation to clinical use. Our findings may reveal valuable in the quest for a blood test for the diagnosis of AD pathology at early disease stages.

List of abbreviations

Aβ1-42 = β-amyloid 1-42

AD = Alzheimer disease

ANGT = Angiotensinogen

APOE = Apolipoprotein E

APOM = Apolipoprotein M

AUC = Area under the curve

CDR = Clinical dementia rating

CERU = Ceruloplasmin

CO7 = Complement component C7

CRP = C-reactive protein

CSF = Cerebrospinal fluid

IBP2 = Insulin-like growth factor-binding protein 2

K0753 = Uncharacterized protein KIAA0753, reviewed as protein moonraker (MOONR)

LASSO = Least absolute shrinkage and selection operator regression

LC = Liquid Chromatography

MCI = Mild cognitive impairment

MS/MS = Tandem mass spectrometry

NOE1 = Noelin

OVCH1 = Ovochymase-1

P-tau181 = Tau phosphorylated at threonine 181

PZP = Pregnancy zone protein

ROC = Receiver operating characteristic

SEPP1 = Selenoprotein P

SHBG = Sex hormone-binding globulin

Acknowledgments. This study was supported by grants from the Swiss National Research Foundation to Dr. Popp (SNF 320030_141179) and funding from the Nestlé Institute of Health Sciences.

Conflict of Interest/Disclosure Statement. Dr. Dayon, Mr. Núñez Galindo, Mr. Corthésy, Dr. Cominetti, and Dr. Migliavacca are employees of Nestlé Institute of Health Sciences S.A.. Dr. Oikonomidi, and Dr. Henry report no disclosures. Dr. Wojcik is an employee

and shareholder of Quartz Bio S.A. and received consultation honoraria from Nestlé Institute of Health Sciences. Dr. Bowman is an employee of Nestlé Institute of Health Sciences S.A., an unpaid scientific advisor of the H2020 EU-funded project PROPAG-AGEING that aims at identifying new molecular signatures for early diagnosis of Parkinson's disease, an editorial board member of the Journal of Alzheimer's Disease (2009-present), and receives research support from the NIH/NIA related to cognitive decline. Dr. Popp received consultation honoraria from Nestlé Institute of Health Sciences.

Author's contributions. Dr. Dayon - study concept and design, acquisition of data, analysis of proteomic data, interpretation of the statistical analysis, and writing of the manuscript. Dr. Wojcik - study concept and design, statistical analysis plan, statistical analysis, interpretation of the statistical analysis, and drafting of the statistical analysis section. Mr. Núñez Galindo - acquisition of data and critical revision of the manuscript. Mr. Corthésy - acquisition of data and critical revision of the manuscript. Dr. Cominetti - analysis of proteomic data and critical revision of the manuscript. Dr. Migliavacca - statistical analysis plan, interpretation of the statistical analysis, and critical revision of the manuscript. Dr. Oikonomidi - acquisition of data and critical revision of the manuscript. Dr. Henry - supervision of data acquisition and critical revision of the manuscript. Dr. Bowman - study concept and design, statistical analysis plan, interpretation of the statistical analysis, critical revision of the manuscript, and overall study supervision. Dr. Popp - study concept and design, interpretation of the statistical analysis, critical revision of the manuscript, and overall study supervision. All authors have given approval to the final version of the manuscript.

References

[1] Prince M, Bryce R, Albanese E, Wimo A, Ribeiro W, Ferri CP (2013) The global prevalence of dementia: A systematic review and metaanalysis. *Alzheimers Dement* **9**, 63-75.

[2] Musiek ES, Holtzman DM (2015) Three dimensions of the amyloid hypothesis: Time, space and 'wingmen'. *Nat Neurosci* **18**, 800-806.

[3] Dubois B, Feldman HH, Jacova C, Hampel H, Molinuevo JL, Blennow K, Dekosky ST, Gauthier S, Selkoe D, Bateman R, Cappa S, Crutch S, Engelborghs S, Frisoni GB, Fox NC, Galasko D, Habert MO, Jicha GA, Nordberg A, Pasquier F, Rabinovici G, Robert P, Rowe C, Salloway S, Sarazin M, Epelbaum S, de Souza LC, Vellas B, Visser PJ, Schneider L, Stern Y, Scheltens P, Cummings JL (2014) Advancing research diagnostic criteria for Alzheimer's disease: The IWG-2 criteria. *Lancet Neurol* **13**, 614-629.

[4] Sperling RA, Aisen PS, Beckett LA, Bennett DA, Craft S, Fagan AM, Iwatsubo T, Jack Jr CR, Kaye J, Montine TJ, Park DC, Reiman EM, Rowe CC, Siemers E, Stern Y, Yaffe K, Carrillo MC, Thies B, Morrison-Bogorad M, Wagster MV, Phelps CH (2011) Toward defining the preclinical stages of Alzheimer's disease: Recommendations from the National Institute on Aging-Alzheimer's Association workgroups on diagnostic guidelines for Alzheimer's disease. *Alzheimers Dement* **7**, 280-292.

[5] Henriksen K, O'Bryant SE, Hampel H, Trojanowski JQ, Montine TJ, Jeromin A, Blennow K, Lönneborg A, Wyss-Coray T, Soares H, Bazenet C, Sjögren M, Hu W, Lovestone S, Karsdal MA, Weiner MW (2014) The future of blood-based biomarkers for Alzheimer's disease. *Alzheimers Dement* **10**, 115-131.

[6] Lista S, Faltraco F, Prvulovic D, Hampel H (2013) Blood and plasma-based proteomic biomarker research in Alzheimer's disease. *Prog Neurobiol* **101-102**, 1-17.

[7] Baird AL, Westwood S, Lovestone S (2015) Blood-based proteomic biomarkers of Alzheimer's disease pathology. *Front Neurol* **6**, 236.

[8] Jack CR, Knopman DS, Jagust WJ, Petersen RC, Weiner MW, Aisen PS, Shaw LM, Vemuri P, Wiste HJ, Weigand SD, Lesnick TG, Pankratz VS, Donohue MC, Trojanowski JQ (2013) Tracking pathophysiological processes in Alzheimer's disease: An updated hypothetical model of dynamic biomarkers. *Lancet Neurol* **12**, 207-216.

[9] Jansen WJ, Ossenkoppele R, Knol DL, Tijms BM, Scheltens P, Verhey FRJ, Visser PJ, Aalten P, Aarsland D, Alcolea D, Alexander M, Almdahl IS, Arnold SE, Baldeiras I, Barthel H, Van Berckel BNM, Bibeau K, Blennow K, Brooks DJ, Van Buchem MA, Camus V, Cavedo E, Chen K, Chetelat G, Cohen AD, Drzezga A, Engelborghs S, Fagan AM, Fladby T, Fleisher AS, Van Der Flier WM, Ford L, Forster S, Fortea J, Foskett N, Frederiksen KS, Freund-Levi Y, Frisoni GB, Froelich L, Gabryelewicz T, Gill KD, Gkatzima O, Gomez-Tortosa E, Gordon MF, Grimmer T, Hampel H, Hausner L, Hellwig S, Herukka SK, Hildebrandt H, Ishihara L, Ivanoiu A, Jagust WJ, Johannsen P, Kandimalla R, Kapaki E, Klimkowicz-Mrowiec A, Klunk WE, Kohler S, Koglin N, Kornhuber J, Kramberger MG, Van Laere K, Landau SM, Lee DY, De Leon M, Lisetti V, Lleo A, Madsen K, Maier W, Marcusson J, Mattsson N, De Mendonca A, Meulenbroek O, Meyer PT, Mintun MA, Mok V, Molinuevo JL, Mollergard HM, Morris JC, Mroczko B, Van Der Mussele S, Na DL, Newberg A, Nordberg A, Nordlund A, Novak GP, Paraskevas GP, Parnetti L, Perera G, Peters O, Popp J, Prabhakar S, Rabinovici GD, Ramakers IHGB, Rami L, De Oliveira CR, Rinne JO, Rodrigue KM, Rodriguez-Rodriguez E, Roe CM, Rot U, Rowe CC, Ruther E, Sabri O, Sanchez-Juan P, Santana I, Sarazin M, Schroder J, Schutte C, Seo SW, Soetewey F, Soininen H, Spiru L, Struyfs H, Teunissen CE, Tsolaki M, Vandenberghe R, Verbeek MM, Villemagne VL, Vos SJB, Van Waalwijk Van Doorn LJC, Waldemar G, Wallin

A, Wallin AK, Wiltfang J, Wolk DA, Zboch M, Zetterberg H (2015) Prevalence of cerebral amyloid pathology in persons without dementia: A meta-analysis. *JAMA* **313**, 1924-1938.

[10] Dayon L, Núñez Galindo A, Corthésy J, Cominetti O, Kussmann M (2014) Comprehensive and scalable highly automated MS-based proteomic workflow for clinical biomarker discovery in human plasma. *J Proteome Res* **13**, 3837-3845.

[11] Cominetti O, Núñez Galindo A, Corthésy J, Oller Moreno S, Irincheeva I, Valsesia A, Astrup A, Saris WHM, Hager J, Kussmann M, Dayon L (2016) Proteomic Biomarker Discovery in 1000 Human Plasma Samples with Mass Spectrometry. *J Proteome Res* **15**, 389-399.

[12] Popp J, Oikonomidi A, Tautvydaitė D, Dayon L, Bacher M, Migliavacca E, Henry H, Kirkland R, Severin I, Wojcik J, Bowman GL (2017) Markers of neuroinflammation associated with Alzheimer's disease pathology in older adults. *Brain Behav Immun* **62**, 203-211.

[13] Morris JC (1993) The clinical dementia rating (cdr): Current version and scoring rules. *Neurology* **43**, 2412-2414.

[14] Winblad B, Palmer K, Kivipelto M, Jelic V, Fratiglioni L, Wahlund LO, Nordberg A, Bäckman L, Albert M, Almkvist O, Arai H, Basun H, Blennow K, De Leon M, Decarli C, Erkinjuntti T, Giacobini E, Graff C, Hardy J, Jack C, Jorm A, Ritchie K, Van Duijn C, Visser P, Petersen RC (2004) Mild cognitive impairment - Beyond controversies, towards a consensus: Report of the International Working Group on Mild Cognitive Impairment. *J Intern Med* **256**, 240-246.

[15] McKhann GM, Knopman DS, Chertkow H, Hyman BT, Jack Jr CR, Kawas CH, Klunk WE, Koroshetz WJ, Manly JJ, Mayeux R, Mohs RC, Morris JC, Rossor MN, Scheltens P, Carrillo MC, Thies B, Weintraub S, Phelps CH (2011) The diagnosis of dementia due to Alzheimer's disease: Recommendations from the National Institute on Aging-Alzheimer's

Association workgroups on diagnostic guidelines for Alzheimer's disease. *Alzheimers Dement* **7**, 263-269.

[16] Buschke H, Sliwinski MJ, Kuslansky G, Lipton RB (1997) Diagnosis of early dementia by the Double Memory Test: Encoding specificity improves diagnostic sensitivity and specificity. *Neurology* **48**, 989-997.

[17] Folstein MF, Folstein SE, McHugh PR (1975) "Mini-mental state". A practical method for grading the cognitive state of patients for the clinician. *J Psychiatr Res* **12**, 189-198.

[18] Zigmond AS, Snaith RP (1983) The Hospital Anxiety and Depression Scale. *Acta Psychiatr Scand* **67**, 361-370.

[19] Jorm AF, Jacomb PA (1989) The Informant Questionnaire on Cognitive Decline in the Elderly (IQCODE): Socio-demographic correlates, reliability, validity and some norms. *Psychol Med* **19**, 1015-1022.

[20] Popp J, Riad M, Freymann K, Jessen F (2007) Diagnostic lumbar puncture performed in the outpatient setting of a memory clinic: Frequency and risk factors of post-lumbar puncture headache. *Nervenarzt* **78**, 547-551.

[21] Tautvydaitė D, Antonietti JP, Henry H, von Gunten A, Popp J (2017) Relations between personality changes and cerebrospinal fluid biomarkers of Alzheimer's disease pathology. *J Psychiatr Res* **90**, 12-20.

[22] Duits FH, Teunissen CE, Bouwman FH, Visser PJ, Mattsson N, Zetterberg H, Blennow K, Hansson O, Minthon L, Andreasen N, Marcusson J, Wallin A, Rikkert MO, Tsolaki M, Parnetti L, Herukka SK, Hampel H, De Leon MJ, Schröder J, Aarsland D, Blankenstein MA, Scheltens P, Van Der Flier WM (2014) The cerebrospinal fluid "alzheimer profile": Easily said, but what does it mean? *Alzheimers Dement* **10**, 713-723.

[23] Youden WJ (1950) Index for rating diagnostic tests. *Cancer* **3**, 32-35.

[24] Dayon L, Sanchez JC (2012) in *Methods in Molecular Biology*, ed. Katrin M, pp. 115-127.

[25] Tibshirani R (2011) Regression shrinkage and selection via the lasso: A retrospective. *J R Stat Soc Series B Stat Methodol* **73**, 273-282.

[26] Friedman J, Hastie T, Tibshirani R (2010) Regularization paths for generalized linear models via coordinate descent. *J Stat Softw* **33**, 1-22.

[27] Robin X, Turck N, Hainard A, Tiberti N, Lisacek F, Sanchez JC, Müller M (2011) pROC: An open-source package for R and S+ to analyze and compare ROC curves. *BMC Bioinform* **12**, 77.

[28] DeLong ER, DeLong DM, Clarke-Pearson DL (1988) Comparing the areas under two or more correlated receiver operating characteristic curves: a nonparametric approach. *Biometrics* **44**, 837-845.

[29] Gauher S Is your Classification Model making lucky guesses? 2016. http://blog.revolutionanalytics.com/2016/03/classification-models.html. Accessed 15 June 2017.

[30] Uhlén M, Fagerberg L, Hallström BM, Lindskog C, Oksvold P, Mardinoglu A, Sivertsson Å, Kampf C, Sjöstedt E, Asplund A, Olsson I, Edlund K, Lundberg E, Navani S, Szigyarto CAK, Odeberg J, Djureinovic D, Takanen JO, Hober S, Alm T, Edqvist PH, Berling H, Tegel H, Mulder J, Rockberg J, Nilsson P, Schwenk JM, Hamsten M, Von Feilitzen K, Forsberg M, Persson L, Johansson F, Zwahlen M, Von Heijne G, Nielsen J, Pontén F (2015) Tissue-based map of the human proteome. *Science* **347**, 1260419.

[31] Oller Moreno S, Cominetti O, Núñez Galindo A, Irincheeva I, Corthésy J, Astrup A, Saris WH, Hager J, Kussmann M, Dayon L (2017) The differential plasma proteome of obese and overweight individuals undergoing a nutritional weight loss and maintenance intervention. *Proteomics Clin Appl*, DOI: 10.1002/prca.201600150.

[32] Huynh RA, Mohan C (2017) Alzheimer's disease: Biomarkers in the genome, blood, and cerebrospinal fluid. *Front Neurol* **8**, 102.

[33] Fernandez AM, Torres-Alemán I (2012) The many faces of insulin-like peptide signalling in the brain. *Nat Rev Neurosci* **13**, 225-239.

[34] Åberg D, Johansson P, Isgaard J, Wallin A, Johansson JO, Andreasson U, Blennow K, Zetterberg H, Åberg ND, Svensson J, Baker L (2015) Increased Cerebrospinal Fluid Level of Insulin-like Growth Factor-II in Male Patients with Alzheimer's Disease. *J Alzheimers Dis* **48**, 637-646.

[35] Hertze J, Nägga K, Minthon L, Hansson O (2014) Changes in cerebrospinal fluid and blood plasma levels of IGF-II and its binding proteins in Alzheimer's disease: An observational study. *BMC Neurol* **14**, 64.

[36] Doecke JD, Laws SM, Faux NG, Wilson W, Burnham SC, Lam CP, Mondal A, Bedo J, Bush AI, Brown B, De Ruyck K, Ellis KA, Fowler C, Gupta VB, Head R, Macaulay SL, Pertile K, Rowe CC, Rembach A, Rodrigues M, Rumble R, Szoeke C, Taddei K, Taddei T, Trounson B, Ames D, Masters CL, Martins RN (2012) Blood-based protein biomarkers for diagnosis of Alzheimer disease. *Arch Neurol* **69**, 1318-1325.

[37] Toledo JB, Da X, Bhatt P, Wolk DA, Arnold SE, Shaw LM, Trojanowski JQ, Davatzikos C (2013) Relationship between Plasma Analytes and SPARE-AD Defined Brain Atrophy Patterns in ADNI. *PLoS One* **8**, e55531.

[38] Lane EM, Hohman TJ, Jefferson AL, For The Alzheimer' SDNI (2016) Insulin-like growth factor binding protein-2 interactions with Alzheimer's disease biomarkers. *Brain Imaging Behav*, 1-8.

[39] Kolev MV, Ruseva MM, Harris CL, Morgan BP, Donev RM (2009) Implication of complement system and its regulators in alzheimer's disease. *Curr Neuropharmacol* **7**, 1-8.

[40] Hong S, Beja-Glasser VF, Nfonoyim BM, Frouin A, Li S, Ramakrishnan S, Merry KM, Shi Q, Rosenthal A, Barres BA, Lemere CA, Selkoe DJ, Stevens B (2016) Complement and microglia mediate early synapse loss in Alzheimer mouse models. *Science* **352**, 712-716.

[41] McGeer PL, McGeer EG (2002) The possible role of complement activation in Alzheimer disease. *Trends Mol Med* **8**, 519-523.

[42] Barembaum M, Moreno TA, LaBonne C, Sechrist J, Bronner-Fraser M (2000) Noelin-1 is a secreted glycoprotein involved in generation of the neural crest. *Nat Cell Biol* **2**, 219-225.

[43] Gupta VB, Laws SM, Villemagne VL, Ames D, Bush AI, Ellis KA, Lui JK, Masters C, Rowe CC, Szoeke C, Taddei K, Martins RN (2011) Plasma apolipoprotein e and Alzheimer disease risk: The AIBL study of aging. *Neurology* **76**, 1091-1098.

[44] Rasmussen KL, Tybjærg-Hansen A, Nordestgaard BG, Frikke-Schmidt R (2015) Plasma levels of apolipoprotein E and risk of dementia in the general population. *Ann Neurol* **77**, 301-311.

[45] Thambisetty M, Tripaldi R, Riddoch-Contreras J, Hye A, An Y, Campbell J, Sojkova J, Kinsey A, Lynham S, Zhou Y, Ferrucci L, Wong DF, Lovestone S, Resnick SM (2010) Proteome-based plasma markers of brain amyloid-β deposition in non-demented older individuals. *J Alzheimers Dis* **22**, 1099-1109.

[46] Luo G, Zhang X, Nilsson-Ehle P, Xu N (2004) Apolipoprotein M. *Lipids Health Dis* **3**, 21.

[47] Kabbara A, Payet N, Cottel D, Frigard B, Amouyel P, Lambert JC (2004) Exclusion of CYP46 and APOM as candidate genes for Alzheimer's disease in a French population. *Neurosci Lett* **363**, 139-143.

[48] Khoonsari E, Häggmark A, Lonnberg M, Mikus M, Kilander L, Lannfelt L, Bergquist J, Ingelsson M, Nilsson P, Kultima K, Shevchenko G (2016) Analysis of the cerebrospinal fluid proteome in Alzheimer's disease payam. *PLoS One* **11**, e0150672.

[49] Bellinger FP, He QP, Bellinger MT, Lin Y, Raman AV, White LR, Berry MJ (2008) Association of selenoprotein P with Alzheimer's pathology in human cortex. *J Alzheimers Dis* **15**, 465-472.

[50] Takemoto AS, Berry MJ, Bellinger FP (2010) Role of selenoprotein P in Alzheimer's disease. *Ethn Dis* **20**, S1-92-95.

[51] Brewer GJ, Kanzer SH, Zimmerman EA, Celmins DF, Heckman SM, Dick R (2010) Copper and ceruloplasmin abnormalities in Alzheimers disease. *Am J Alzheimers Dis Other Demen* **25**, 490-497.

[52] Snaedal J, Kristinsson J, Gunnarsdóttir S, Ólafsdóttir Á, Baldvinsson M, Jóhannesson T (1998) Copper, ceruloplasmin and superoxide dismutase in patients with Alzheimer's disease. A case-control study. *Dementia Geriatr Cogn Disord* **9**, 239-242.

[53] Kessler H, Pajonk FG, Meisser P, Schneider-Axmann T, Hoffmann KH, Supprian T, Herrmann W, Obeid R, Multhaup G, Falkai P, Bayer TA (2006) Cerebrospinal fluid diagnostic markers correlate with lower plasma copper and ceruloplasmin in patients with Alzheimer's disease. *J Neural Transm* **113**, 1763-1769.

[54] Park JH, Lee DW, Park KS (2014) Elevated serum copper and ceruloplasmin levels in Alzheimer's disease. *Asia Pac Psychiatry* **6**, 38-45.

[55] Wyss-Coray T, Rogers J (2012) Inflammation in Alzheimer disease-A brief review of the basic science and clinical literature. *Cold Spring Harb Perspect Med* **2**, a006346.

[56] Edwards M, Balldin VH, Hall J, O'Bryant S (2015) Molecular markers of neuropsychological functioning and Alzheimer's disease. *Alzheimers Dement Diagn Assess Dis Monit* **1**, 61-66.

[57] Nilsson K, Gustafson L, Hultberg B (2011) C-reactive protein level is decreased in patients with Alzheimer's disease and related to cognitive function and survival time. *Clin Biochem* **44**, 1205-1208.

[58] O'Bryant SE, Waring SC, Hobson V, Hall JR, Moore CB, Bottiglieri T, Massman P, Diaz-Arrastia R (2010) Decreased C-reactive protein levels in alzheimer disease. *J Geriatr Psychiatry Neurol* **23**, 49-53.

[59] Yarchoan M, Louneva N, Xie SX, Swenson FJ, Hu W, Soares H, Trojanowski JQ, Lee VMY, Kling MA, Shaw LM, Chen-Plotkin A, Wolk DA, Arnold SE (2013) Association of plasma C-reactive protein levels with the diagnosis of Alzheimer's disease. *J Neurol Sci* **333**, 9-12.

[60] Ijsselstijn L, Dekker LJM, Stingl C, Van Der Weiden MM, Hofman A, Kros JM, Koudstaal PJ, Sillevis Smitt PAE, Ikram MA, Breteler MMB, Luider TM (2011) Serum levels of pregnancy zone protein are elevated in presymptomatic alzheimer's disease. *J Proteome Res* **10**, 4902-4910.

[61] Muller M, Schupf N, Manly JJ, Mayeux R, Luchsinger JA (2010) Sex hormone binding globulin and incident Alzheimer's disease in elderly men and women. *Neurobiol Aging* **31**, 1758-1765.

[62] Xu J, Xia LL, Song N, Chen SD, Wang G (2016) Testosterone, estradiol, and sex hormone-binding globulin in Alzheimer’s disease: A meta-analysis. *Curr Alzheimer Res* **13**, 215-222.

[63] Mateos L, Ismail MAM, Gil-Bea FJ, Leoni V, Winblad B, Björkhem I, Cedazo-Mínguez A (2011) Upregulation of brain renin angiotensin system by 27-hydroxycholesterol in Alzheimer's disease. *J Alzheimers Dis* **24**, 669-679.

FIGURE CAPTIONS

Figure 1. ROC curves of the models including plasma proteins for classification of non-AD *versus* AD CSF biomarker profiles (*i.e.*, P-tau181/Aβ1-42 ≤ 0.0779 and P-tau181/Aβ1-42 > 0.0779 respectively) in all subjects (**A**) and in subjects with cognitive impairment (**B**). In the whole cohort, the best model for AD CSF profile classification contains APOE, CO7, IBP2, and NOE1 in addition of age and presence of APOE ε4 allele; the reference model to outperform is composed of age and presence of APOE ε4 allele. In subjects with cognitive impairment, the best model for AD CSF profile classification contains ANGT, APOC2, APOM, CAH2 [#], CC180, CO7, CO8G, FIBB, HBA, HXA3, IBP2, ICAM2, K0753, NOE1, OVCH1, PZP, SAMP, SEPP1, and TSP1[#] in addition of presence of APOE ε4 allele; the reference model to outperform is composed of age, gender, years of education, and presence of APOE ε4 allele. The opacity of the curves is proportional to the accuracy of the models. The diamonds indicate the selected most accurate models. The *p*-values on the graphs indicate the significance of the differences of AUC.

Figure 2. ROC curves of the model including plasma proteins predictive of CSF Aβ1-42 levels (**A**). The best model is composed of CADH5, CERU, CO4B, CO7, CRP, FA12, FHR1, GNPTG, HGFL, IBP2, IPSP, K0753, KPYM [#], OVCH1, RET4, and SHBG in addition of age and presence of APOE ε4 allele; the reference model contains age, gender, years of education, and presence of APOE ε4 allele. The opacity of the curves is proportional to the accuracy of the models. The diamonds indicate the selected most accurate models. The *p*-value on the graphs indicates the significance of the differences of AUC. Box-plots of plasma proteins according to CSF Aβ1-42 levels, *i.e.*, "low" when [Aβ1-42] < 724 pg/ml and "high" when Aβ1-42] ≥ 724 pg/ml for positive and negative CSF profiles of amyloid pathology, respectively (**B**). Relative protein fold change ratios were used. Level of significant is indicated as *p*-value after Bonferroni correction.

Figure 3. Comparison of protein panels determined with LASSO for the classification of AD CSF biomarker profile in the whole sample and subset with cognitive impairment (**A**). Comparison of protein panels determined with LASSO for the classification of AD pathology and amyloidosis CSF-defined profiles (**B**).

Table 1. Demographics and clinical characteristics.

	P-tau181/ Aβ1-42 ≤ 0.0779 (*n* = 78)	**P-tau181/ Aβ1-42 > 0.0779 (*n* = 42)**	**[Aβ1-42] ≥ 724 pg/mL (*n* = 73)**	**[Aβ1-42] < 724 pg/mL (*n* = 47)**	**CDR = 0 (*n* = 48)**	**CDR > 0 (*n* = 72)**
Age (years), mean (SD)	68.4 (8.3)	74.1 (5.6)*	68.1 (8.2)	73.9 (6.1)*	66.0 (7.4)	73.3 (6.9)*
Gender, No. (%) of Males	25 (32.05%)	18 (42.86%)	26 (35.62%)	17 (36.17%)	17 (35.42%)	26 (36.11%)
Education years, mean (SD)	12.5 (2.7)	12.1 (2.4)	12.6 (2.7)	12.0 (2.5)	13.2 (2.3)	11.8 (2.7)*
CDR, score (% of subjects)	0 (60.2%) or 0.5 (37.2%) or 1 (2.6%)	0 (2.4%) or 0.5 (80.9%) or 1 (16.7%)	0 (57.6%) or 0.5 (39.7%) or 1 (2.7%)	0 (12.8%) or 0.5 (72.3%) or 1 (14.9%)	0 (100%)	0.5 (87.5%) or 1 (12.5%)
MMSE scale, mean (SD)	27.8 (2.3)	25.2 (3.7)*	27.8 (2.2)	25.6 (3.8)*	28.5 (1.4)	25.9 (3.5)*
APOE ε4 carriers, No. (%)	13 (16.67%)	24 (57.14%)*	10 (13.70%)	27 (57.45%)*	11 (22.92%)	26 (36.11%)*
CSF Aβ1-42 (pg/mL), mean (SD)	979.9 (196.4)	601.2 (190.0)*	1026.1 (160.1)	569.9 (111.1)*	957.4 (194.0)	774.0 (281.5)*
CSF tau (pg/mL) , mean (SD)	235.1 (104.2)	624.2 (322.4)*	268.2 (155.6)	531.4 (346.1)*	221.5 (82.9)	471.1 (316.6)*
CSF P-tau181 (pg/mL), mean (SD)	46.7 (13.4)	90.3 (44.8)*	51.3 (18.8)	78.6 (46.9)*	45.9 (13.3)	72.7 (40.9)*
P-tau181/Aβ1-42, mean (SD)	0.05 (0.01)	0.16 (0.10)*	0.05 (0.02)	0.15 (0.11)*	0.049 (0.015)	0.114 (0.097)*
AD CSF profile, No. (%) of subjects	0 (0.0%)	42 (100.0%)*	4 (5.48%)	38 (80.85%)*	1 (2.08%)	41 (56.94%)*
Amyloid pathology CSF profile, No. (%) of subjects	9 (11.54%)	38 (90.48%)*	0 (0.0%)	47 (100.0%)*	6 (12.50%)	41 (56.94%)*
CSF albumin index, mean (SD)	5.9 (2.4)	6.4 (2.3)	5.9 (2.5)	6.4 (2.2)	5.3 (1.9)	6.6 (2.5)*

*statistically different ($p \leq 0.05$) from P-tau181/Aβ1-42 ≤ 0.0779, [Aβ1-42] ≥ 724 pg/mL, and CDR = 0, respectively, using *t*-tests for continuous variables and binomial proportion tests for categorical variables. CSF albumin index = [CSF albumin] / [serum albumin] × 100; MMSE = Mini Mental State Examination

Table 2. Performance of classification models.

	Reference models	Best models
AD CSF profile		
Accuracy	78.3%	80.5%
Sensitivity	50.0%	61.9%
Specificity	93.6%	90.8%
AUC	0.83 [0.74-0.90])	0.88 [0.81-0.93]
AD CSF profile in cognitive impairment		
Accuracy	77.8%	88.9%
Sensitivity	82.9%	85.4%
Specificity	71.0%	93.6%
AUC	0.83 [0.73-0.91]	0.96 [0.90-0.99]*
Amyloid pathology CSF profile		
Accuracy	80.0%	92.4%*
Sensitivity	82.2%	93.0%
Specificity	76.6%	91.5%
AUC	0.86 [0.78-0.92]	0.96 [0.93-0.99]*

*statistically different ($p \leq 0.05$) from reference model using a McNemar test (accuracy) or a bootstrap test (AUC). Sensitivity and specificity are given for the most accurate models. For AUC, 95% confidence intervals are given.

Figure 1.

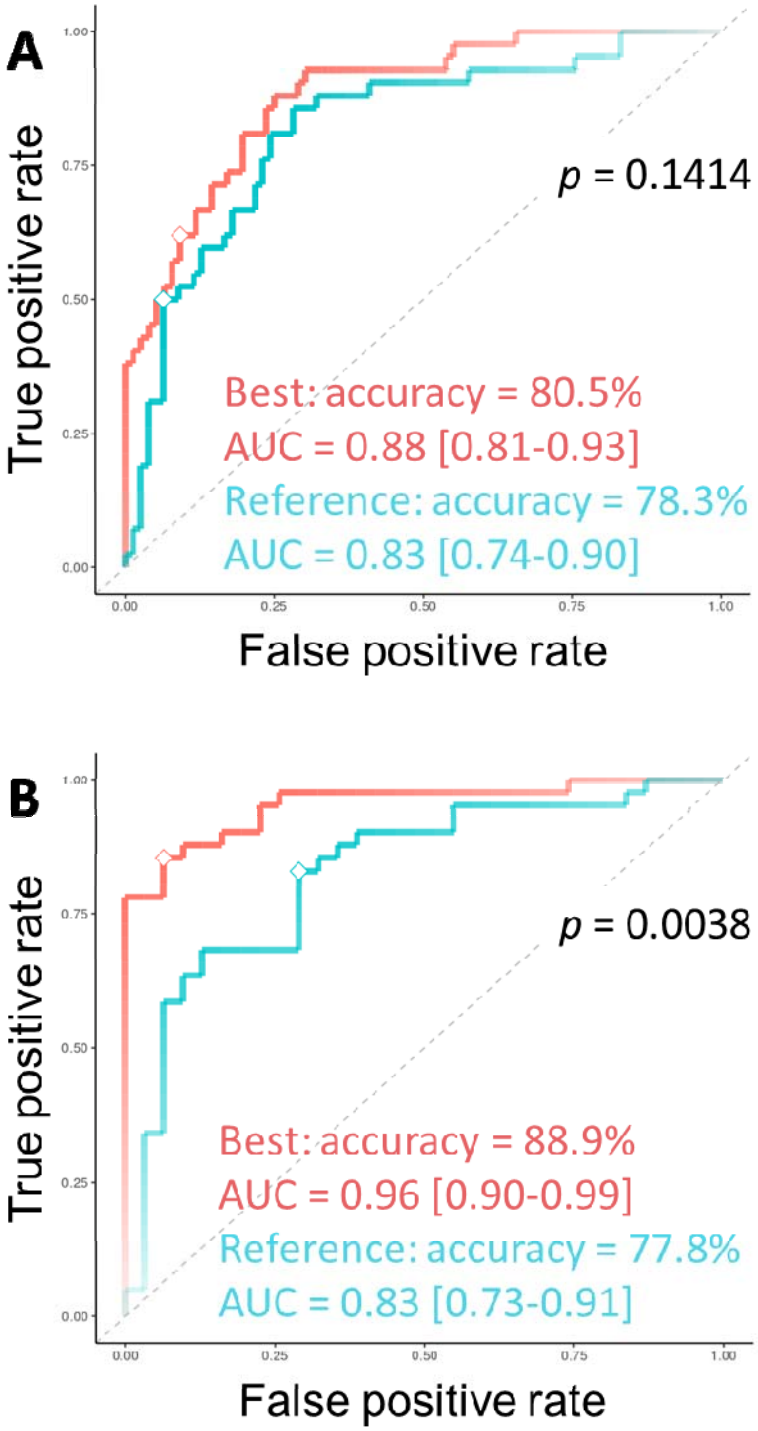
A
True positive rate
False positive rate
p = 0.1414
Best: accuracy = 80.5%
AUC = 0.88 [0.81-0.93]
Reference: accuracy = 78.3%
AUC = 0.83 [0.74-0.90]
B
True positive rate
False positive rate
p = 0.0038
Best: accuracy = 88.9%
AUC = 0.96 [0.90-0.99]
Reference: accuracy = 77.8%
AUC = 0.83 [0.73-0.91]

Figure 2.

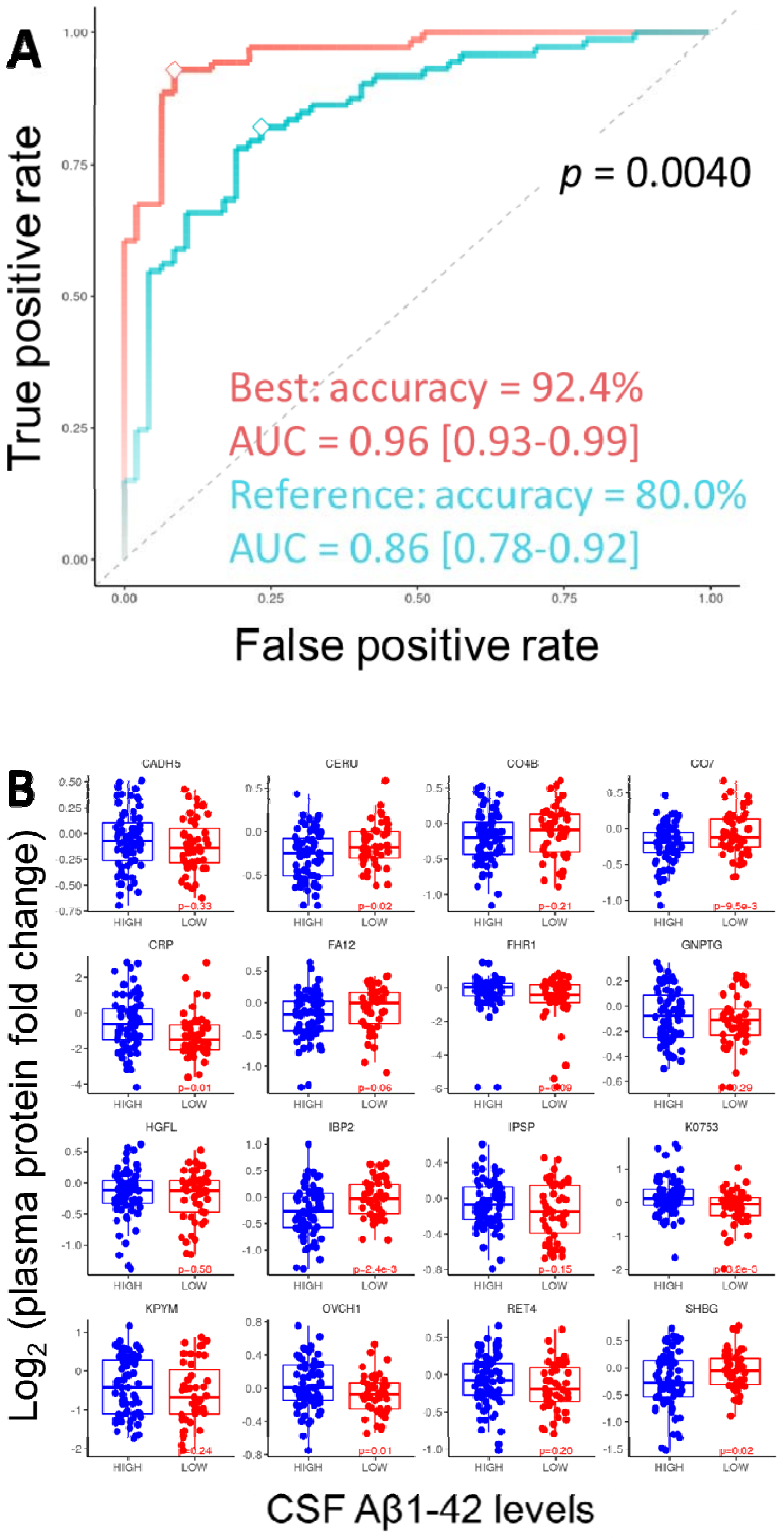
A
True positive rate
False positive rate
p = 0.0040
Best: accuracy = 92.4%
AUC = 0.96 [0.93-0.99]
Reference: accuracy = 80.0%
AUC = 0.86 [0.78-0.92]
B
Log2 (plasma protein fold change)
CSF Aβ1-42 levels
CADH5
CERU
CO4B
CO7
CRP
FA12
FHR1
GNPTG
HGFL
IBP2
IPSP
K0753
KPYM
OVCH1
RET4
SHBG
HIGH
LOW

Figure 3.

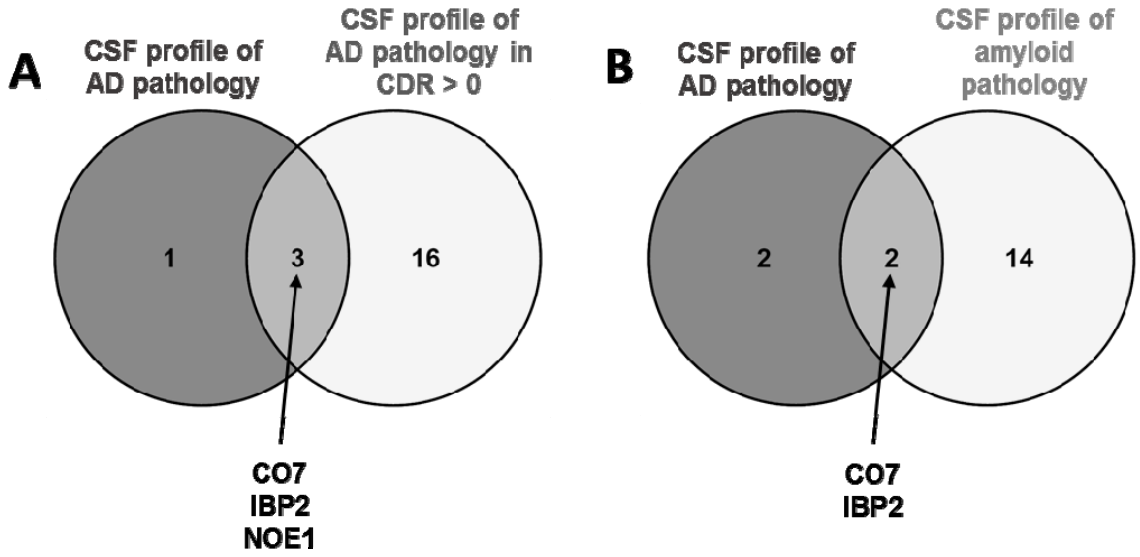
A
CSF profile of AD pathology
CSF profile of AD pathology in CDR > 0
1
3
16
CO7
IBP2
NOE1
B
CSF profile of AD pathology
CSF profile of amyloid pathology
2
2
14
CO7
IBP2

Supplementary Material

Plasma proteomic profiles of CSF-defined Alzheimer pathology in older adults

Loïc Dayon[1, *], Jérôme Wojcik[2], Antonio Núñez Galindo[1], John Corthésy[1], Ornella Cominetti[1], Aikaterini Oikonomidi[3], Hugues Henry[4], Eugenia Migliavacca[1], Gene L. Bowman[1], and Julius Popp[3]

[1]Nestlé Institute of Health Sciences, Lausanne, Switzerland
[2]Quartz Bio, Geneva, Switzerland
[3]CHUV, Old Age Psychiatry, Department of Psychiatry, Lausanne, Switzerland
[4]CHUV, Department of Laboratories, Lausanne, Switzerland

Correspondence to: *Nestlé Institute of Health Sciences, EPFL Innovation Park, Bâtiment H, 1015 Lausanne, Switzerland; Email: loic.dayon@rd.nestle.com, Phone: +41 21 632 6114, Fax: +41 21 632 6499

SUPPLEMENTARY TABLE

Table TS1. Quality-controlled plasma proteins measured with MS. The proteins indicated in bold are part of at least one of the best models that include plasma protein measurements.

Entry	Entry name	Protein name	*n*	Number of missing values	Mean	SD	Median	AD CSF profile	AD CSF profile in cognitive impairment	Amyloid pathology CSF profile
P04217	A1BG_HUMAN	Alpha-1B-glycoprotein	118	0	-0.1518	0.2242	-0.1538			
P08697	A2AP_HUMAN	Alpha-2-antiplasmin	118	0	-0.0644	0.2241	-0.0566			
P02750	A2GL_HUMAN	Leucine-rich alpha-2-glycoprotein	118	0	-0.1847	0.3656	-0.1302			
P01011	AACT_HUMAN	Alpha-1-antichymotrypsin	118	0	-0.1366	0.2297	-0.1264			
P62736[#]	ACTA_HUMAN[#]	Actin, aortic smooth muscle[#]	118	0	-0.8926	0.9408	-0.9313			
P60709[#]	ACTB_HUMAN[#]	Actin, cytoplasmic 1[#]	118	0	-0.7556	0.7864	-0.8273			
Q15848	ADIPO_HUMAN	Adiponectin	118	0	-0.1318	0.3529	-0.1083			
P43652	AFAM_HUMAN	Afamin	118	0	-0.1617	0.2902	-0.1819			
P35858	ALS_HUMAN	Insulin-like growth factor-binding protein complex acid labile subunit	118	0	-0.1687	0.3041	-0.1663			
P02760	AMBP_HUMAN	Protein AMBP	118	0	-0.1523	0.2384	-0.1741			
P15144	AMPN_HUMAN	Aminopeptidase N	118	0	-0.09203	0.3349	-0.1177			
P03950	ANGI_HUMAN	Angiogenin	118	0	-0.1655	0.2811	-0.2067			
Q9Y5C1	ANGL3_HUMAN	Angiopoietin-related protein 3	118	0	-0.08084	0.3301	-0.1187			
P01019	**ANGT_HUMAN**	**Angiotensinogen**	**118**	**0**	**-0.1393**	**0.2643**	**-0.1367**		×	
P01008	ANT3_HUMAN	Antithrombin-III	118	0	-0.1446	0.2074	-0.1739			
P02647	APOA1_HUMAN	Apolipoprotein A-I	115	3	-0.4764	0.5642	-0.5486			
P02652	APOA2_HUMAN	Apolipoprotein A-II	118	0	-0.398	0.9283	-0.5566			
P06727	APOA4_HUMAN	Apolipoprotein A-IV	118	0	-0.1459	0.4276	-0.12			
P08519	APOA_HUMAN	Apolipoprotein	118	0	-0.9064	1.58	-1.172			
P04114	APOB_HUMAN	Apolipoprotein B-100	118	0	-0.118	0.4624	-0.107			

P02655	**APOC2_HUMAN**	**Apolipoprotein C-II**	**118**	**0**	**0.2051**	**0.7714**	**0.1695**		×	
P02656	APOC3_HUMAN	Apolipoprotein C-III	118	0	0.1312	0.7042	0.1513			
P55056	APOC4_HUMAN	Apolipoprotein C-IV	118	0	-0.05639	0.7286	-0.07604			
P05090	APOD_HUMAN	Apolipoprotein D	118	0	-0.1206	0.302	-0.112			
P02649	**APOE_HUMAN**	**Apolipoprotein E**	**118**	**0**	**-0.04135**	**0.4088**	**-0.07157**	×		
P02749	APOH_HUMAN	Beta-2-glycoprotein 1	118	0	-0.1341	0.2946	-0.1676			
O14791	APOL1_HUMAN	Apolipoprotein L1	118	0	-0.1713	0.4537	-0.1916			
O95445	**APOM_HUMAN**	**Apolipoprotein M**	**118**	**0**	**-0.1481**	**0.4373**	**-0.1748**		×	
P61160[#]	ARP2_HUMAN[#]	Actin-related protein 2[#]	118	0	-0.9501	1.132	-0.8938			
P07307	ASGR2_HUMAN	Asialoglycoprotein receptor 2	118	0	-0.09116	0.3854	-0.08583			
O75882	ATRN_HUMAN	Attractin	118	0	-0.131	0.2614	-0.09691			
Q76LX8	ATS13_HUMAN	A disintegrin and metalloproteinase with thrombospondin motifs 13	118	0	-0.0296	0.2598	-0.04933			
P61769	B2MG_HUMAN	Beta-2-microglobulin	118	0	-0.1901	0.3556	-0.2493			
Q15582	BGH3_HUMAN	Transforming growth factor-beta-induced protein ig-h3	118	0	-0.1258	0.2825	-0.1083			
P43251	BTD_HUMAN	Biotinidase	118	0	-0.1455	0.268	-0.1387			
A2RUR9	C144A_HUMAN	Coiled-coil domain-containing protein 144A	118	0	-0.2292	0.3097	-0.2742			
P02745	C1QA_HUMAN	Complement C1q subcomponent subunit A	118	0	-0.1824	0.3281	-0.1716			
P02746	C1QB_HUMAN	Complement C1q subcomponent subunit B	118	0	-0.1893	0.2599	-0.1929			
P02747	C1QC_HUMAN	Complement C1q subcomponent subunit C	118	0	-0.1872	0.2585	-0.1964			
P00736	C1R_HUMAN	Complement C1r subcomponent	118	0	-0.1348	0.21	-0.1537			
Q9NZP8	C1RL_HUMAN	Complement C1r subcomponent-like protein	118	0	-0.1317	0.2979	-0.1222			
P09871	C1S_HUMAN	Complement C1s subcomponent	118	0	-0.1523	0.2257	-0.185			
P04003	C4BPA_HUMAN	C4b-binding protein alpha chain	118	0	-0.1129	0.4514	-0.1349			
P20851	C4BPB_HUMAN	C4b-binding protein beta chain	118	0	-0.06907	0.4524	-0.0954			
P55290	CAD13_HUMAN	Cadherin-13	118	0	-0.1075	0.2354	-0.08777			×
P33151	**CADH5_HUMAN**	**Cadherin-5**	**118**	**0**	**-0.08321**	**0.2746**	**-0.09096**			

P00915	CAH1_HUMAN	Carbonic anhydrase 1	118	0	-0.2405	0.5714	-0.2995			
P00918[#]	**CAH2_HUMAN**[#]	**Carbonic anhydrase 2**[#]	**118**	**0**	**-0.3351**	**0.6546**	**-0.2994**		×	
P62158[#]	CALM_HUMAN[#]	Calmodulin[#]	118	0	-0.8015	1.216	-0.7403			
Q01518[#]	CAP1_HUMAN[#]	Adenylyl cyclase-associated protein 1[#]	118	0	-0.8465	1.136	-0.8818			
P07339	CATD_HUMAN	Cathepsin D	118	0	-0.1755	0.3626	-0.1893			
P08185	CBG_HUMAN	Corticosteroid-binding globulin	118	0	-0.1337	0.3455	-0.1603			
Q96IY4	CBPB2_HUMAN	Carboxypeptidase B2	118	0	-0.1423	0.2432	-0.1716			
P15169	CBPN_HUMAN	Carboxypeptidase N catalytic chain	118	0	-0.1682	0.2686	-0.1667			
Q9P1Z9	**CC180_HUMAN**	**Coiled-coil domain-containing protein 180**	**114**	**4**	**-0.1388**	**0.4206**	**-0.0854**		×	
P08571	CD14_HUMAN	Monocyte differentiation antigen CD14	118	0	-0.1223	0.2607	-0.1282			
O43866	CD5L_HUMAN	CD5 antigen-like	118	0	-0.3214	0.5788	-0.3355			
P00450	**CERU_HUMAN**	**Ceruloplasmin**	**118**	**0**	**-0.2236**	**0.2735**	**-0.2107**			×
P00751	CFAB_HUMAN	Complement factor B	118	0	-0.1462	0.2818	-0.1384			
P00746	CFAD_HUMAN	Complement factor D	118	0	-0.1408	0.342	-0.1896			
P08603	CFAH_HUMAN	Complement factor H	118	0	-0.2002	0.2767	-0.1923			
P05156	CFAI_HUMAN	Complement factor I	118	0	-0.1472	0.2353	-0.1563			
P06276	CHLE_HUMAN	Cholinesterase	118	0	-0.1762	0.354	-0.1922			
O00299[#]	CLIC1_HUMAN[#]	Chloride intracellular channel protein 1[#]	118	0	-0.6921	1.058	-0.6656			
P10909	CLUS_HUMAN	Clusterin	118	0	-0.008554	0.2332	-0.009325			
Q96KN2	CNDP1_HUMAN	Beta-Ala-His dipeptidase	118	0	-0.1556	0.3449	-0.1666			
P06681	CO2_HUMAN	Complement C2	118	0	-0.1459	0.2201	-0.1523			
P01024	CO3_HUMAN	Complement C3	118	0	-0.2336	0.2465	-0.2393			
P0C0L4	CO4A_HUMAN	Complement C4-A	118	0	-0.2496	0.6239	-0.1126			
P0C0L5	**CO4B_HUMAN**	**Complement C4-B**	**118**	**0**	**-0.1708**	**0.3555**	**-0.146**			×
P01031	CO5_HUMAN	Complement C5	118	0	-0.2247	0.2402	-0.2336			
P13671	CO6_HUMAN	Complement component C6	118	0	-0.1592	0.3223	-0.1377			
P10643	**CO7_HUMAN**	**Complement component C7**	**118**	**0**	**-0.1559**	**0.2957**	**-0.1573**	×	×	×
P07357	CO8A_HUMAN	Complement component C8 alpha chain	118	0	-0.1534	0.2534	-0.1477			
P07358	CO8B_HUMAN	Complement component C8 beta chain	118	0	-0.1242	0.3075	-0.1211			

P07360	**CO8G_HUMAN**	**Complement component C8 gamma chain**	**118**	**0**	**-0.1576**	**0.2355**	**-0.1754**		×	
P02748	CO9_HUMAN	Complement component C9	118	0	-0.1334	0.36	-0.1257			
P23528[#]	COF1_HUMAN[#]	Cofilin-1[#]	118	0	-1.003	1.251	-0.9584			
P39060	COIA1_HUMAN	Collagen alpha-1	118	0	-0.1492	0.2522	-0.1698			
Q9Y6Z7	COL10_HUMAN	Collectin-10	118	0	-0.1091	0.2534	-0.08242			
Q9BWP8	COL11_HUMAN	Collectin-11	118	0	-0.1459	0.2744	-0.1385			
P49747	COMP_HUMAN	Cartilage oligomeric matrix protein	118	0	-0.1243	0.3019	-0.09208			
P22792	CPN2_HUMAN	Carboxypeptidase N subunit 2	118	0	-0.1138	0.296	-0.09341			
Q9NQ79	CRAC1_HUMAN	Cartilage acidic protein 1	118	0	-0.0518	0.3076	-0.07464			
P54108	CRIS3_HUMAN	Cysteine-rich secretory protein 3	118	0	-0.1477	0.3423	-0.1579			
P02741	**CRP_HUMAN**	**C-reactive protein**	**117**	**1**	**-0.8914**	**1.386**	**-1.074**			×
P21291[#]	CSRP1_HUMAN[#]	Cysteine and glycine-rich protein 1[#]	114	4	-0.8139	1.57	-0.6383			
P02775[#]	CXCL7_HUMAN[#]	Platelet basic protein[#]	118	0	-0.8362	1.244	-0.7261			
P01034	CYTC_HUMAN	Cystatin-C	118	0	-0.1499	0.2739	-0.1822			
Q16610	ECM1_HUMAN	Extracellular matrix protein 1	118	0	-0.2994	0.3581	-0.2995			
P06733[#]	ENOA_HUMAN[#]	Alpha-enolase[#]	118	0	-0.4821	0.866	-0.4808			
P00488	F13A_HUMAN	Coagulation factor XIII A chain	118	0	-0.2153	0.2454	-0.214			
P05160	F13B_HUMAN	Coagulation factor XIII B chain	118	0	-0.1506	0.2414	-0.1527			
P00742	FA10_HUMAN	Coagulation factor X	118	0	-0.1199	0.2353	-0.1404			
P03951	FA11_HUMAN	Coagulation factor XI	118	0	-0.1883	0.2411	-0.186			
P00748	**FA12_HUMAN**	**Coagulation factor XII**	**118**	**0**	**-0.1707**	**0.3614**	**-0.1395**			×
P12259	FA5_HUMAN	Coagulation factor V	118	0	-0.04017	0.2813	-0.0711			
P08709	FA7_HUMAN	Coagulation factor VII	114	4	-0.1547	0.3146	-0.1477			
P00740	FA9_HUMAN	Coagulation factor IX	118	0	-0.1338	0.2794	-0.1704			
P23142	FBLN1_HUMAN	Fibulin-1	118	0	-0.135	0.2925	-0.1802			
Q12805	FBLN3_HUMAN	EGF-containing fibulin-like extracellular matrix protein 1	118	0	-0.1428	0.27	-0.1454			
O75636	FCN3_HUMAN	Ficolin-3	118	0	-0.2046	0.4357	-0.2011			
P02765	FETUA_HUMAN	Alpha-2-HS-glycoprotein	118	0	-0.1171	0.2808	-0.1315			
Q9UGM5	FETUB_HUMAN	Fetuin-B	118	0	-0.1394	0.3312	-0.1346			

Q08830	FGL1_HUMAN	Fibrinogen-like protein 1	114	4	-0.07815	0.42	-0.08464			
Q03591	**FHR1_HUMAN**	**Complement factor H-related protein 1**	**117**	**1**	**-0.4268**	**1.266**	**-0.05908**			×
P36980	FHR2_HUMAN	Complement factor H-related protein 2	118	0	-0.2542	0.6162	-0.09342			
Q9BXR6	FHR5_HUMAN	Complement factor H-related protein 5	118	0	-0.1465	0.267	-0.1228			
P02671	FIBA_HUMAN	Fibrinogen alpha chain	118	0	-0.5995	0.5304	-0.5592			
P02675	**FIBB_HUMAN**	**Fibrinogen beta chain**	**118**	**0**	**-0.5894**	**0.5639**	**-0.5503**		×	
P02679	FIBG_HUMAN	Fibrinogen gamma chain	118	0	-0.6337	0.6019	-0.5949			
P02751	FINC_HUMAN	Fibronectin	118	0	-0.6088	0.7327	-0.566			
P04406[#]	G3P_HUMAN[#]	Glyceraldehyde-3-phosphate dehydrogenase[#]	118	0	-0.3645	1.082	-0.3639			
P52566[#]	GDIR2_HUMAN[#]	Rho GDP-dissociation inhibitor 2[#]	118	0	-0.6258	0.9865	-0.5765			
P06396	GELS_HUMAN	Gelsolin	118	0	-0.1283	0.261	-0.111			
Q9UJJ9	**GNPTG_HUMAN**	**N-acetylglucosamine-1-phosphotransferase subunit gamma**	**118**	**0**	**-0.09485**	**0.2113**	**-0.09463**			×
P22352	GPX3_HUMAN	Glutathione peroxidase 3	118	0	-0.1352	0.2293	-0.1305			
P09211	GSTP1_HUMAN	Glutathione S-transferase P	114	4	-0.2787	0.3381	-0.2566			
Q14520	HABP2_HUMAN	Hyaluronan-binding protein 2	118	0	-0.1101	0.2657	-0.1205			
P69905	**HBA_HUMAN**	**Hemoglobin subunit alpha**	**114**	**4**	**-0.01683**	**0.2973**	**-0.0672**		×	
P02790	HEMO_HUMAN	Hemopexin	118	0	-0.1388	0.2269	-0.1405			
P05546	HEP2_HUMAN	Heparin cofactor 2	118	0	-0.0981	0.3049	-0.1071			
Q04756	HGFA_HUMAN	Hepatocyte growth factor activator	118	0	-0.1605	0.2921	-0.1503			
P26927	**HGFL_HUMAN**	**Hepatocyte growth factor-like protein**	**118**	**0**	**-0.1888**	**0.3912**	**-0.1253**			×
P04196	HRG_HUMAN	Histidine-rich glycoprotein	118	0	-0.1975	0.5792	-0.1346			
O43365	**HXA3_HUMAN**	**Homeobox protein Hox-A3**	**118**	**0**	**-0.2561**	**0.6545**	**-0.17**		×	
Q9Y4L1	HYOU1_HUMAN	Hypoxia up-regulated protein 1	118	0	-0.1268	0.2824	-0.1531			
P18065	**IBP2_HUMAN**	**Insulin-like growth factor-binding protein 2**	**118**	**0**	**-0.168**	**0.4467**	**-0.1483**	×	×	×
P17936	IBP3_HUMAN	Insulin-like growth factor-binding protein 3	118	0	-0.1425	0.2407	-0.1517			
P22692	IBP4_HUMAN	Insulin-like growth factor-binding protein 4	118	0	-0.1503	0.251	-0.1787			
P24593	IBP5_HUMAN	Insulin-like growth factor-binding protein	118	0	-0.1176	0.262	-0.1119			

		5								
P05155	IC1_HUMAN	Plasma protease C1 inhibitor	118	0	-0.1862	0.3529	-0.2082			
P13598	**ICAM2_HUMAN**	**Intercellular adhesion molecule 2**	**118**	**0**	**-0.1373**	**0.3186**	**-0.1546**		×	
P01344	IGF2_HUMAN	Insulin-like growth factor II	118	0	-0.1526	0.2928	-0.1431			
Q9NPH3	IL1AP_HUMAN	Interleukin-1 receptor accessory protein	118	0	-0.1134	0.3386	-0.1489			
P55103	INHBC_HUMAN	Inhibin beta C chain	114	4	-0.02429	0.4146	-0.0005375			
P05154	**IPSP_HUMAN**	**Plasma serine protease inhibitor**	**118**	**0**	**-0.09499**	**0.2863**	**-0.1064**			×
P19827	ITIH1_HUMAN	Inter-alpha-trypsin inhibitor heavy chain H1	118	0	-0.1297	0.251	-0.1168			
P19823	ITIH2_HUMAN	Inter-alpha-trypsin inhibitor heavy chain H2	118	0	-0.1461	0.2327	-0.1453			
Q06033	ITIH3_HUMAN	Inter-alpha-trypsin inhibitor heavy chain H3	118	0	-0.1623	0.3844	-0.1926			
Q14624	ITIH4_HUMAN	Inter-alpha-trypsin inhibitor heavy chain H4	118	0	-0.08849	0.2168	-0.1073			
Q2KHM9	**K0753_HUMAN**	**Uncharacterized protein KIAA0753, reviewed as protein moonraker (MOONR_HUMAN)**	**114**	**4**	**0.01047**	**0.5115**	**0.03482**		×	×
P04264	K2C1_HUMAN	Keratin, type II cytoskeletal 1	114	4	-0.1647	0.915	-0.2828			
P29622	KAIN_HUMAN	Kallistatin	118	0	-0.08967	0.2615	-0.1012			
Q96Q89	KI20B_HUMAN	Kinesin-like protein KIF20B	118	0	-0.08375	0.3106	-0.07772			
P03952	KLKB1_HUMAN	Plasma kallikrein	118	0	-0.1745	0.3095	-0.2246			
P01042	KNG1_HUMAN	Kininogen-1	118	0	-0.105	0.1947	-0.1293			
P14618[#]	**KPYM_HUMAN**[#]	**Pyruvate kinase PKM**[#]	**118**	**0**	**-0.4708**	**0.7683**	**-0.5302**			×
P18428	LBP_HUMAN	Lipopolysaccharide-binding protein	118	0	-0.08474	0.4077	-0.09975			
P07195	LDHB_HUMAN	L-lactate dehydrogenase B chain	118	0	-0.2319	0.4322	-0.2658			
Q3ZCW2[#]	LEGL_HUMAN[#]	Galectin-related protein[#]	118	0	-0.3857	0.66	-0.4195			
Q08380	LG3BP_HUMAN	Galectin-3-binding protein	118	0	-0.08951	0.4951	-0.134			
P51884	LUM_HUMAN	Lumican	118	0	-0.1298	0.2862	-0.1048			
P14151	LYAM1_HUMAN	L-selectin	118	0	-0.1712	0.3086	-0.1474			
P61626	LYSC_HUMAN	Lysozyme C	118	0	-0.1888	0.3783	-0.1764			
P33908	MA1A1_HUMAN	Mannosyl-oligosaccharide 1,2-alpha-	118	0	-0.1465	0.233	-0.1515			

		mannosidase IA								
P48740	MASP1_HUMAN	Mannan-binding lectin serine protease 1	118	0	-0.1983	0.2722	-0.2186			
O00187	MASP2_HUMAN	Mannan-binding lectin serine protease 2	118	0	-0.1379	0.272	-0.1364			
P11226	MBL2_HUMAN	Mannose-binding protein C	118	0	-0.2075	0.4558	-0.216			
P20774	MIME_HUMAN	Mimecan	114	4	-0.1021	0.2606	-0.09706			
P08253	MMP2_HUMAN	72 kDa type IV collagenase	118	0	-0.09619	0.2326	-0.1179			
P02144	MYG_HUMAN	Myoglobin	114	4	-0.169	0.3857	-0.1869			
Q9Y2K3	MYH15_HUMAN	Myosin-15	118	0	-0.04519	0.3517	-0.0659			
A7E2Y1	MYH7B_HUMAN	Myosin-7B	118	0	-0.1177	0.3573	-0.1436			
O60524	NEMF_HUMAN	Nuclear export mediator factor NEMF	118	0	-0.1165	0.3251	-0.1679			
Q99784	**NOE1_HUMAN**	**Noelin**	**114**	**4**	**-0.0944**	**0.2525**	**-0.09089**	×	×	
O60287	NPA1P_HUMAN	Nucleolar pre-ribosomal-associated protein 1	118	0	-0.1296	0.3319	-0.1588			
P15559	NQO1_HUMAN	NAD	118	0	-0.04222	0.3003	-0.04605			
Q7RTY7	**OVCH1_HUMAN**	**Ovochymase-1**	**114**	**4**	**-0.003395**	**0.2849**	**-0.03339**		×	×
Q15113	PCOC1_HUMAN	Procollagen C-endopeptidase enhancer 1	118	0	-0.1214	0.3306	-0.0828			
Q8NBP7	PCSK9_HUMAN	Proprotein convertase subtilisin/kexin type 9	114	4	-0.1388	0.3151	-0.1166			
Q9UHG3	PCYOX_HUMAN	Prenylcysteine oxidase 1	118	0	-0.1434	0.3825	-0.19			
O00151[#]	PDLI1_HUMAN[#]	PDZ and LIM domain protein 1[#]	118	0	-0.7868	1.165	-0.854			
P36955	PEDF_HUMAN	Pigment epithelium-derived factor	118	0	-0.1041	0.322	-0.1279			
P12955	PEPD_HUMAN	Xaa-Pro dipeptidase	118	0	-0.2908	0.2427	-0.2779			
P98160	PGBM_HUMAN	Basement membrane-specific heparan sulfate proteoglycan core protein	114	4	-0.1862	0.3053	-0.1938			
P00558	PGK1_HUMAN	Phosphoglycerate kinase 1	118	0	-0.2238	0.5024	-0.1637			
Q96PD5	PGRP2_HUMAN	N-acetylmuramoyl-L-alanine amidase	118	0	-0.1297	0.2547	-0.1187			
P80108	PHLD_HUMAN	Phosphatidylinositol-glycan-specific phospholipase D	118	0	-0.07568	0.378	-0.07594			
Q6UXB8	PI16_HUMAN	Peptidase inhibitor 16	118	0	-0.1626	0.3636	-0.2044			
Q15149	PLEC_HUMAN	Plectin	118	0	-0.01254	0.3024	0.0067			
P08567[#]	PLEK_HUMAN[#]	Pleckstrin[#]	118	0	-0.8932	1.051	-0.838			

P00747	PLMN_HUMAN	Plasminogen	118	0	-0.1637	0.2994	-0.1472			
P13796	PLSL_HUMAN	Plastin-2	118	0	-0.1187	0.2693	-0.137			
P27169	PON1_HUMAN	Serum paraoxonase/arylesterase 1	118	0	-1.048	0.5318	-1.083			
Q15063	POSTN_HUMAN	Periostin	118	0	-0.1076	0.3567	-0.04761			
P62937[#]	PPIA_HUMAN[#]	Peptidyl-prolyl cis-trans isomerase A[#]	118	0	-0.9648	1.183	-0.9656			
P23284[#]	PPIB_HUMAN[#]	Peptidyl-prolyl cis-trans isomerase B[#]	118	0	-0.7734	0.7855	-0.7952			
P32119	PRDX2_HUMAN	Peroxiredoxin-2	118	0	-0.3327	0.6442	-0.3301			
P30041[#]	PRDX6_HUMAN[#]	Peroxiredoxin-6[#]	118	0	-0.4302	1.002	-0.4722			
Q92954	PRG4_HUMAN	Proteoglycan 4	118	0	-0.1398	0.3626	-0.1317			
P04070	PROC_HUMAN	Vitamin K-dependent protein C	118	0	-0.1145	0.2622	-0.1298			
P07737[#]	PROF1_HUMAN[#]	Profilin-1[#]	118	0	-0.7663	1.078	-0.784			
P27918	PROP_HUMAN	Properdin	118	0	-0.1697	0.2658	-0.1698			
P07225	PROS_HUMAN	Vitamin K-dependent protein S	118	0	-0.06697	0.2691	-0.05886			
P22891	PROZ_HUMAN	Vitamin K-dependent protein Z	118	0	-0.2003	0.5999	-0.1461			
P41222	PTGDS_HUMAN	Prostaglandin-H2 D-isomerase	118	0	-0.1551	0.289	-0.175			
P20742	**PZP_HUMAN**	**Pregnancy zone protein**	**118**	**0**	**-0.3128**	**0.7697**	**-0.2925**		×	
O00391	QSOX1_HUMAN	Sulfhydryl oxidase 1	118	0	-0.1126	0.2062	-0.1112			
Q99969	RARR2_HUMAN	Retinoic acid receptor responder protein 2	118	0	-0.1616	0.3342	-0.1567			
P05451	REG1A_HUMAN	Lithostathine-1-alpha	118	0	-0.1451	0.4334	-0.139			
P02753	**RET4_HUMAN**	**Retinol-binding protein 4**	**118**	**0**	**-0.116**	**0.3363**	**-0.1002**			×
Q53QZ3	RHG15_HUMAN	Rho GTPase-activating protein 15	118	0	-0.1917	0.2767	-0.1897			
P07998	RNAS1_HUMAN	Ribonuclease pancreatic	118	0	-0.1842	0.4214	-0.216			
P34096	RNAS4_HUMAN	Ribonuclease 4	118	0	-0.1609	0.2556	-0.184			
P62979[#]	RS27A_HUMAN[#]	Ubiquitin-40S ribosomal protein S27a[#]	118	0	-0.6083	0.6899	-0.6866			
P06703[#]	S10A6_HUMAN[#]	Protein S100-A6[#]	118	0	-0.3874	0.7144	-0.4101			
P05109	S10A8_HUMAN	Protein S100-A8	118	0	-0.4547	0.7919	-0.5549			
P06702	S10A9_HUMAN	Protein S100-A9	118	0	-0.4377	0.725	-0.559			
P0DJI8	SAA1_HUMAN	Serum amyloid A-1 protein	118	0	-0.1987	0.8143	-0.2453			
P02743	**SAMP_HUMAN**	**Serum amyloid P-component**	**118**	**0**	**-0.3371**	**0.4685**	**-0.3659**		×	

P49908	**SEPP1_HUMAN**	**Selenoprotein P**	**118**	**0**	**-0.06431**	**0.2893**	**-0.098**		×	
Q7Z333	SETX_HUMAN	Probable helicase senataxin	114	4	-0.113	0.2729	-0.1068			
O75368[#]	SH3L1_HUMAN[#]	SH3 domain-binding glutamic acid-rich-like protein[#]	118	0	-0.4995	0.8764	-0.5311			
Q9H299[#]	SH3L3_HUMAN[#]	SH3 domain-binding glutamic acid-rich-like protein 3[#]	118	0	-0.7534	1.124	-0.6808			
P04278	**SHBG_HUMAN**	**Sex hormone-binding globulin**	**118**	**0**	**-0.1564**	**0.4752**	**-0.1705**			×
P03973	SLPI_HUMAN	Antileukoproteinase	118	0	-0.107	0.3078	-0.1069			
P00441[#]	SODC_HUMAN[#]	Superoxide dismutase [Cu-Zn] [#]	118	0	-0.4151	0.5544	-0.4349			
Q13103	SPP24_HUMAN	Secreted phosphoprotein 24	118	0	0.1501	0.5418	0.159			
P11277	SPTB1_HUMAN	Spectrin beta chain, erythrocytic	114	4	-0.05267	0.4516	0.001725			
Q01082	SPTB2_HUMAN	Spectrin beta chain, non-erythrocytic 1	118	0	-0.1329	0.4151	-0.09646			
Q96C24	SYTL4_HUMAN	Synaptotagmin-like protein 4	118	0	-0.06331	0.2124	-0.04308			
P37840[#]	SYUA_HUMAN[#]	Alpha-synuclein[#]	118	0	-0.3043	0.8879	-0.402			
P37802[#]	TAGL2_HUMAN[#]	Transgelin-2[#]	118	0	-0.8592	1.152	-0.7877			
Q9BYX2	TBD2A_HUMAN	TBC1 domain family member 2A	118	0	-0.1357	0.3085	-0.1599			
P22105	TENX_HUMAN	Tenascin-X	114	4	-0.1479	0.2728	-0.173			
P05452	TETN_HUMAN	Tetranectin	118	0	-0.1094	0.2036	-0.1			
P05543	THBG_HUMAN	Thyroxine-binding globulin	118	0	-0.1437	0.2296	-0.1585			
P10599[#]	THIO_HUMAN[#]	Thioredoxin[#]	118	0	-0.3641	0.7664	-0.4164			
P00734	THRB_HUMAN	Prothrombin	118	0	-0.1221	0.2311	-0.1406			
P01033	TIMP1_HUMAN	Metalloproteinase inhibitor 1	118	0	-0.1756	0.3414	-0.1835			
P16035	TIMP2_HUMAN	Metalloproteinase inhibitor 2	118	0	-0.1121	0.2401	-0.1435			
Q8WZ42	TITIN_HUMAN	Titin	118	0	-0.1687	0.2159	-0.1726			
Q9Y490[#]	TLN1_HUMAN[#]	Talin-1[#]	118	0	-0.4711	0.7136	-0.4417			
P67936[#]	TPM4_HUMAN[#]	Tropomyosin alpha-4 chain[#]	118	0	-1.061	1.209	-1.086			
P07996[#]	**TSP1_HUMAN[#]**	**Thrombospondin-1[#]**	**118**	**0**	**-0.4236**	**0.7338**	**-0.4406**		×	
P02766	TTHY_HUMAN	Transthyretin	118	0	-0.004292	0.6448	0.009837			
P62328[#]	TYB4_HUMAN[#]	Thymosin beta-4[#]	118	0	-0.968	1.572	-0.6693			
Q86UX7	URP2_HUMAN[#]	Fermitin family homolog 3[#]	118	0	-0.3894	0.6739	-0.3669			

Q6EMK4	VASN_HUMAN	Vasorin	118	0	-0.1229	0.2018	-0.1061			
P18206[#]	VINC_HUMAN[#]	Vinculin[#]	118	0	-0.5185	0.6759	-0.5553			
P02774	VTDB_HUMAN	Vitamin D-binding protein	118	0	-0.1591	0.2739	-0.152			
P04004	VTNC_HUMAN	Vitronectin	118	0	-0.1224	0.2932	-0.142			
P04275	VWF_HUMAN	von Willebrand factor	118	0	-0.2175	0.4241	-0.2522			
P25311	ZA2G_HUMAN	Zinc-alpha-2-glycoprotein	118	0	-0.1529	0.3407	-0.1625			
Q9UK55	ZPI_HUMAN	Protein Z-dependent protease inhibitor	118	0	-0.1289	0.3055	-0.1162			
Q15942[#]	ZYX_HUMAN[#]	Zyxin[#]	118	0	-0.5832	0.9187	-0.5192			
P63104[#]	1433Z_HUMAN[#]	14-3-3 protein zeta/delta[#]	118	0	-0.805	0.9321	-0.7811			

SUPPLEMENTARY FIGURES

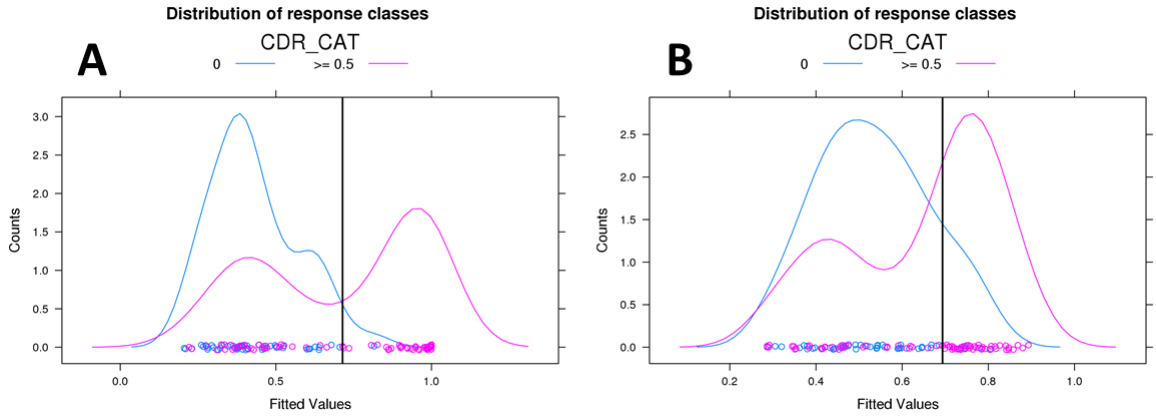

Figure S1. Supervised determination of CSF P-tau181/Aβ1-42 (A) and Aβ1-42 (B) cutoffs from the 48 healthy volunteers with normal cognition and 72 memory clinic patients with MCI or mild dementia of AD type. The vertical black lines indicate the fitted value that maximized the Youden index (= sensitivity + specificity - 1) in the ROC analysis predicting CDR categories (CDR = 0 *versus* CDR > 0). It corresponds to a cutoff of 0.0779 and 724 pg/mL for CSF P-tau181/Aβ1-42 ratio and CSF Aβ1-42 concentration, respectively.

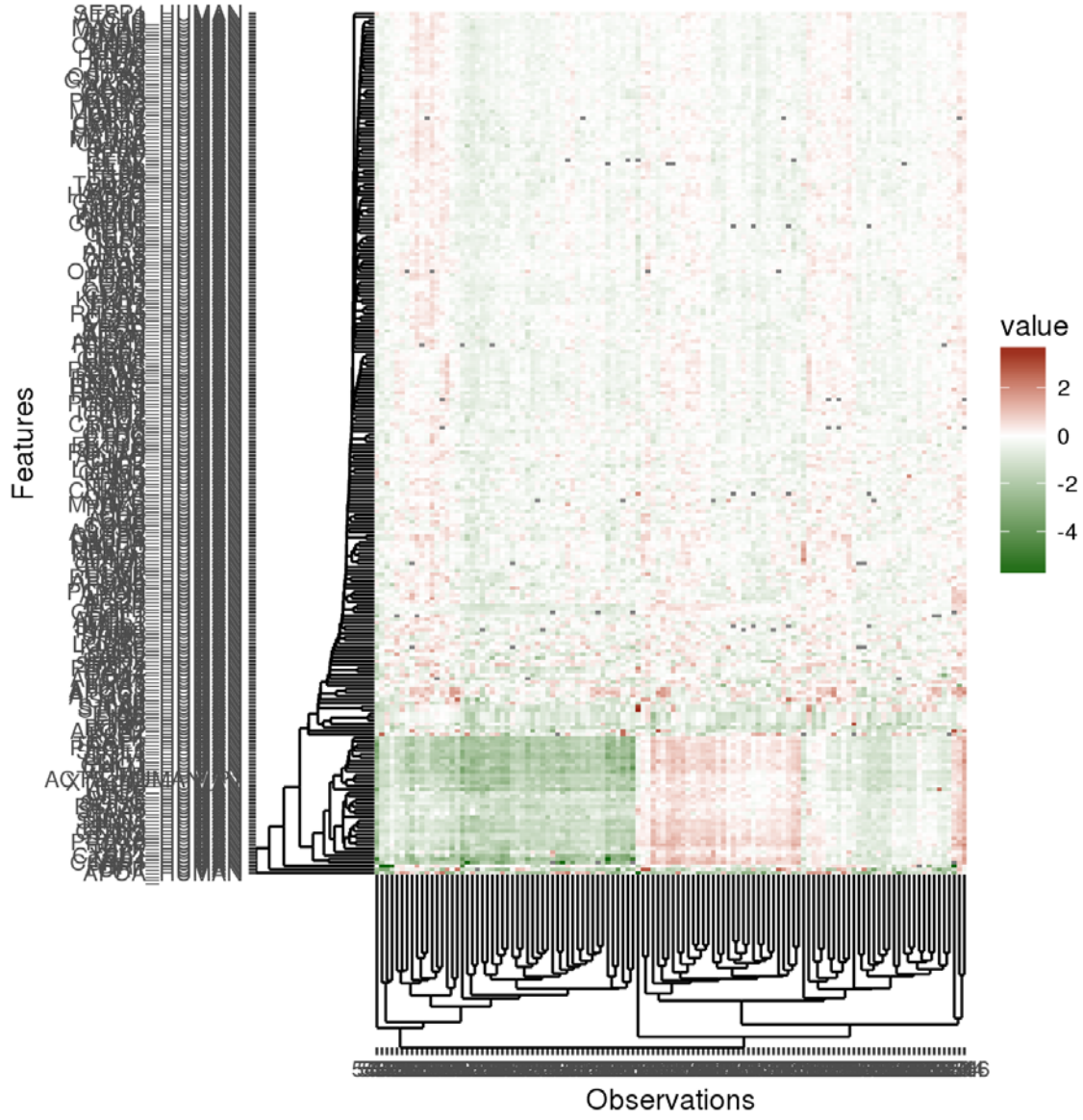

Figure S2. Heatmap of plasma proteome profiles after hierarchical clustering. Features = proteins; Observations = samples.

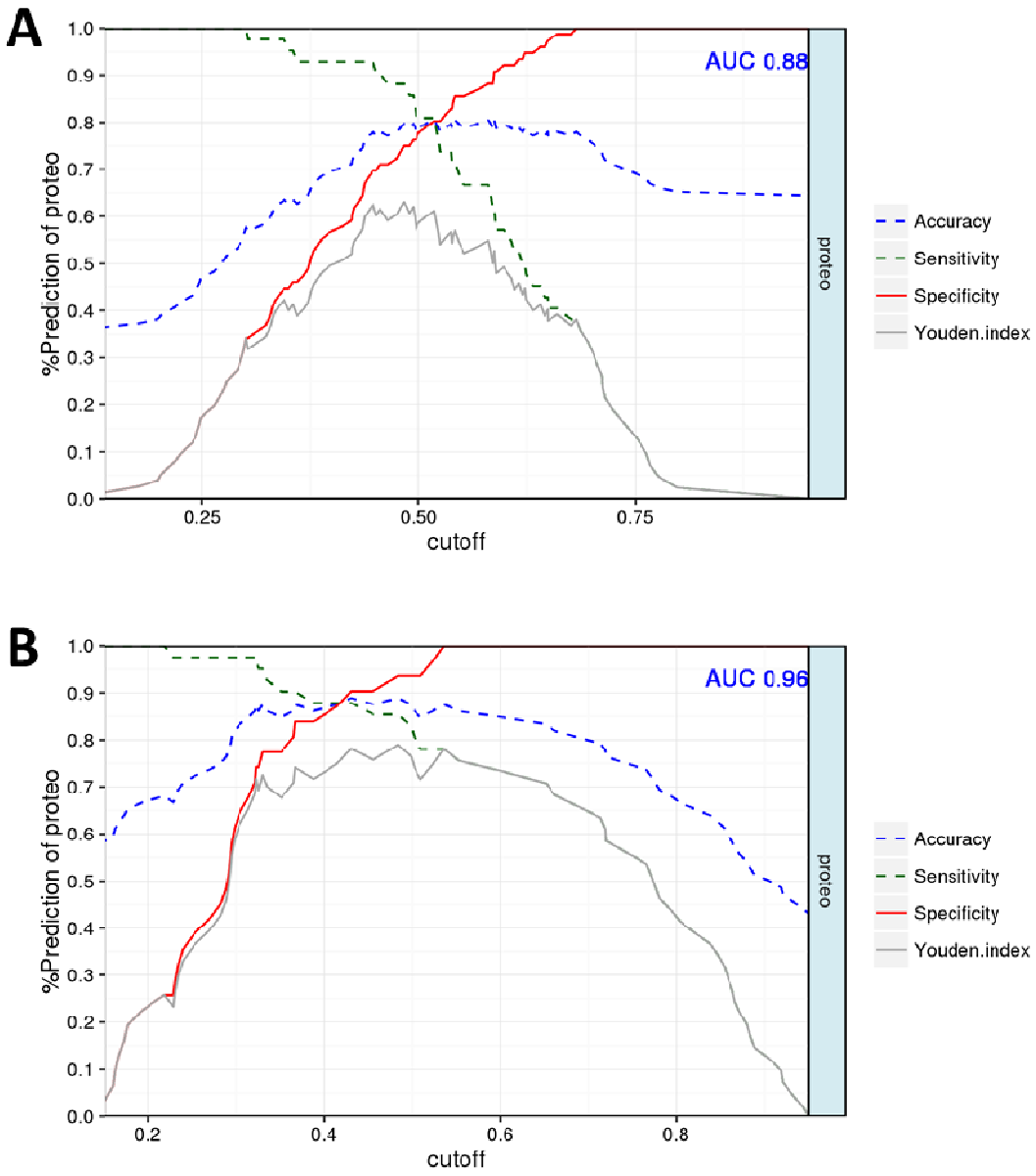

Figure S3. Plot displaying the sensitivities, specificities, Youden indexes, and accuracies of all possible cutoffs of the models including plasma proteins for classification of non-AD *versus* AD CSF biomarker profiles (i.e., P-tau181/Aβ1-42 ≤ 0.0779 and P-tau181/Aβ1-42 > 0.0779 respectively) in all subjects (**A**) and in subjects with cognitive impairment (**B**).

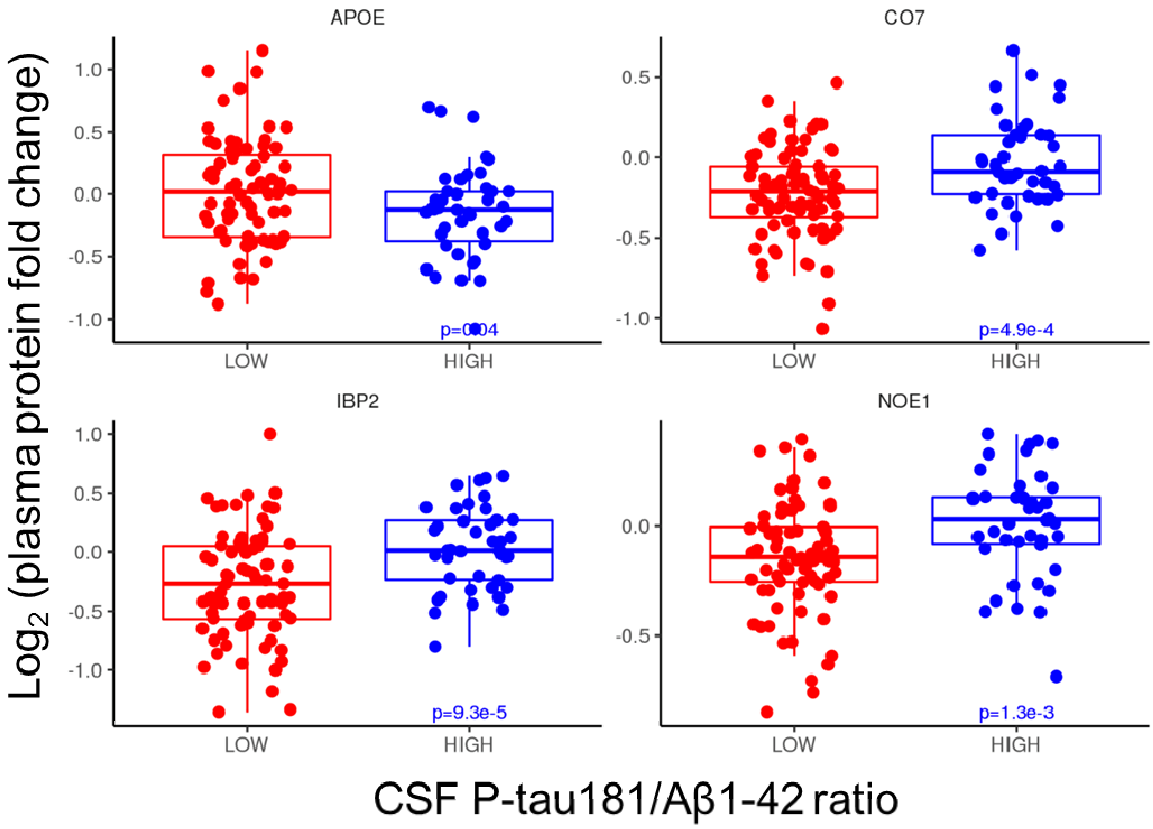

Figure S4. Box-plots of plasma proteins according to CSF P-tau181/Aβ1-42 ratio, *i.e.*, "low" when P-tau181/Aβ1-42 ≤ 0.0779 and "high" when P-tau181/Aβ1-42 > 0.0779 for negative and positive CSF profiles of AD pathology, respectively. Relative protein fold change ratios were used. Level of significant is indicated as *p*-value after Bonferroni correction.

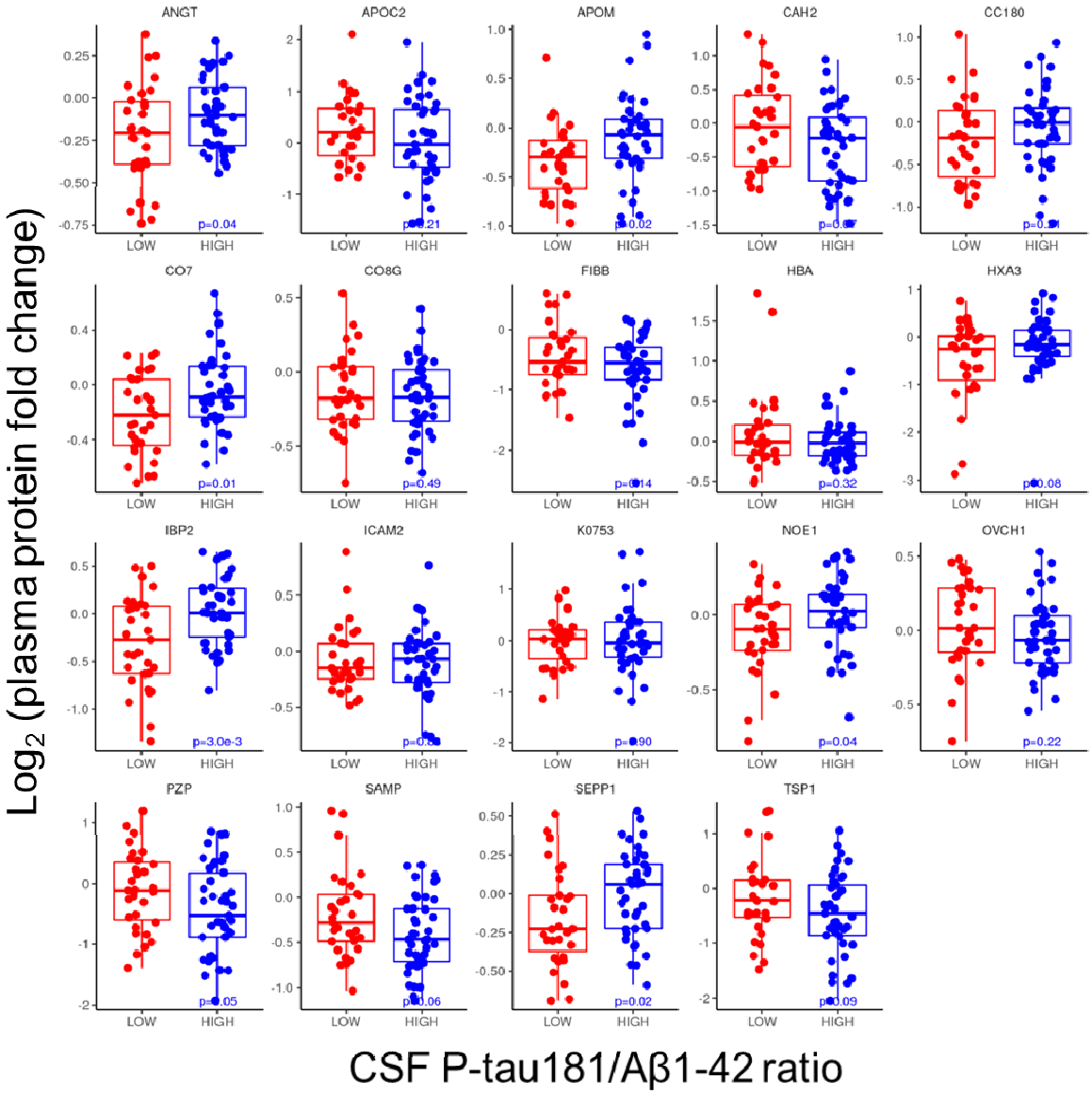

Figure S5. Box-plots of plasma proteins in cognitive impairment (*i.e.*, subset of individuals with CDR > 0) according to CSF P-tau181/Aβ1-42 ratio, *i.e.*, "low" when P-tau181/Aβ1-42 ≤ 0.0779 and "high" when P-tau181/Aβ1-42 > 0.0779 for negative and positive CSF profiles of AD pathology, respectively. Relative protein fold change ratios were used. Level of significant is indicated as *p*-value after Bonferroni correction.

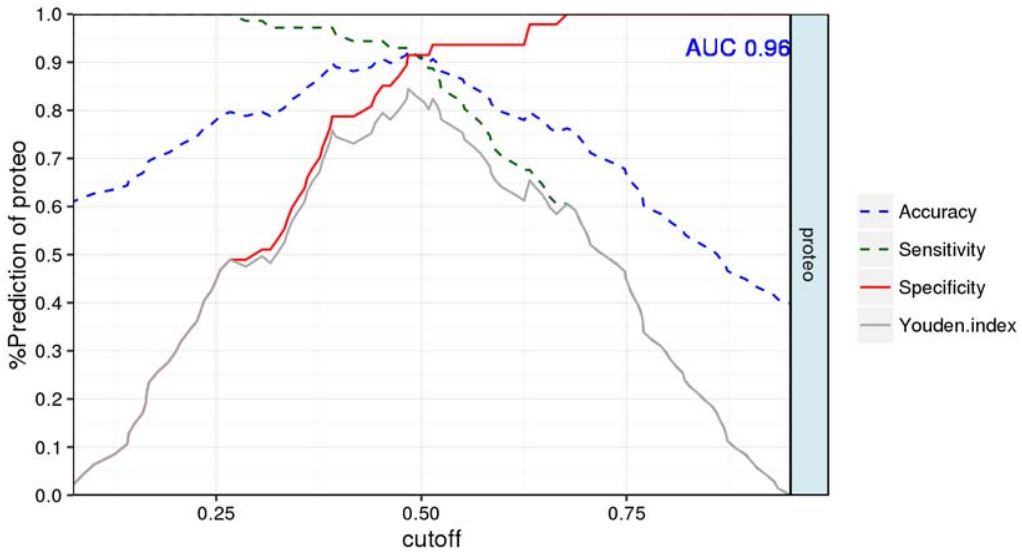

Figure S6. Plot displaying the sensitivities, specificities, Youden indexes, and accuracies of all possible cutoffs of the model including plasma proteins predictive of CSF Aβ1-42 levels**.**

SUPPLEMENTARY METHODS

Materials. Iodoacetamide (IAA), tris(2-carboxyethyl) phosphine hydrochloride (TCEP), triethylammonium hydrogen carbonate buffer 1 M pH = 8.5, sodium dodecyl sulfate, and β-lactoglobulin (LACB) from bovine milk were purchased from Sigma (St. Louis, MO, USA). Formic acid (FA, 99%) and CH_3CN were from BDH (VWR International Ltd., Poole, UK). Hydroxylamine solution 50 *wt* % in H_2O (99.999%) was acquired from Aldrich (Milwaukee, WI, USA). H_2O (18.2 MΩ·cm at 25 °C) was obtained from a Milli-Q apparatus (Millipore, Billerica, MA, USA). Trifluoroacetic acid Uvasol® was sourced from Merck Millipore (Billerica, MA, USA). The 6-plex TMTs [24] were purchased from Thermo Scientific (Rockford, IL, USA). Sequencing grade modified Lys-C/trypsin was procured from Promega (Madison, WI, USA). For immuno-affinity depletion of 14 abundant human proteins, multiple affinity removal system (MARS) columns, Buffer A, and Buffer B were obtained from Agilent Technologies (Wilmington, DE, USA). Oasis HLB cartridges (1cc, 30 mg) were acquired from Waters (Milford, MA, USA) and Strata-X 33u Polymeric reversed-phase (RP) and Strata-X-C 33u Polymeric strong cation-exchange (SCX) solid-phase extraction (SPE) cartridges (30 mg/1 mL) from Phenomenex (Torrance, CA, USA).

Sample preparation for proteomic analysis. From 25 µL of each plasma sample (diluted in 75 µL of Buffer A containing 0.0134 $mg \cdot mL^{-1}$ LACB and filtered with 0.22 µm filter plate from Millipore), 14 abundant plasma proteins were removed, following the manufacturer instructions, with MARS columns and high performance liquid chromatography (HPLC) systems (Thermo Scientific, San Jose, CA, USA) equipped with an HTC-PAL (CTC Analytics AG, Zwingen, Switzerland) fraction collectors. After immuno-depletion, samples were snap-freezed and stored at -80 °C. Buffer exchange was performed with RP cartridges mounted on a 96-hole holder and a vacuum manifold, as previously described [10]. Samples were subsequently evaporated with a

vacuum centrifuge (Thermo Scientific) and stored at -80 °C. Reduction with TCEP, alkylation with IAA, digestion with Lys-C/trypsin, TMT 6-plex labeling, sample pooling, and SPE purification (Oasis HLB and SCX) were performed on a 4-channels Microlab Star liquid handler (Hamilton, Bonaduz, Switzerland) according to a previously reported protocol [10]. The pooled 6-plex TMT-labeled samples were then evaporated to dryness before storage at -80 °C.

Reversed-phase liquid chromatography tandem mass spectrometry. The samples were dissolved in 500 µL H_2O/CH_3CN/FA 96.9/3/0.1 for RP liquid chromatography tandem mass spectrometry (LC MS/MS). RP-LC MS/MS was performed with hybrid linear ion trap-Orbitrap (LTQ-OT) Elite and an Ultimate 3000 RSLC nano system (Thermo Scientific) as recently described [10]. Proteolytic peptides (injection of 5 µL of sample) were trapped on an Acclaim PepMap 75 µm × 2 cm (C18, 3 µm, 100 Å) pre-column and separated on an Acclaim PepMap RSLC 75 µm × 50 cm (C18, 2 µm, 100 Å) column (Thermo Scientific) coupled to a stainless steel nanobore emitter (40 mm, OD 1/32") mounted on a Nanospray Flex Ion Source (Thermo Scientific). The analytical separation was run for 150 min using a gradient that reached 30% of CH_3CN after 140 min and 80% of CH_3CN after 150 min at a flow rate of 220 $nL \cdot min^{-1}$. For MS survey scans, the OT resolution was 120000 (ion population of 1×10^6) with an *m/z* window from 300 to 1500. For MS/MS with higher-energy collisional dissociation (HCD) at 35% of the normalized collision energy, ion population was set to 1×10^5 (isolation width of 2), with a resolution of 15000, first mass at *m/z* = 100, and a maximum injection time of 250 ms in the OT. A maximum of 10 precursor ions (most intense) were selected for MS/MS. Dynamic exclusion was set for 60 seconds within a ± 5 ppm window. A lock mass of *m/z* = 445.1200 was used. Each sample was analyzed in duplicate.

Data analysis. Proteome Discoverer (version 1.4, Thermo Scientific) was used as data analysis interface. Identification was performed against the human UniProtKB/Swiss-Prot database

(08/12/2014 release) including the LACB sequence (20194 sequences in total). Mascot (version 2.4.2, Matrix Science, London, UK) was used. Variable amino acid modifications were oxidized methionine, deamidated asparagine/glutamine, and 6-plex TMT-labeled peptide amino terminus (+ 229.163 Da). 6-plex TMT-labeled lysine (+ 229.163 Da) was set as fixed modifications as well as carbamidomethylation of cysteine. Trypsin was selected as the proteolytic enzyme, with a maximum of two potential missed cleavages. Peptide and fragment ion tolerance were set to, respectively, 10 ppm and 0.02 Da. All Mascot result files were loaded into Scaffold Q+S 4.4.1.1 (Proteome Software, Portland, OR, USA) to be further searched with X! Tandem (version CYCLONE (2010.12.01.1)). Both peptide and protein FDRs were fixed at 1% maximum, with a 2 unique peptide criterion to report protein identification. Quantitative values were exported from Scaffold Q+S as log2 of the protein ratio fold changes with respect to their measurements in the biological reference, *i.e.*, mean log2 values after isotopic purity correction but without normalization applied between samples and experiments. The biological reference was a pool of all individual plasma samples labelled with 6-plex TMT reporter-ions at *m/z* = 126 and 131, allowing ratio fold change calculation with respect to both channels. Because of the concordance between both calculation results, the average of the values was done as well as the average of both replicate measurements.

CSF Aβ1-42, tau, and P-tau181. CSF Aβ1-42, total-tau (tau), and tau phosphorylated at threonine 181 (P-tau181) concentrations were measured using commercially available ELISA kits (Fujirebio, Ghent, Belgium).

APOE genotyping. DNA was extracted from whole blood using the QIAsymphony DSP DNA Kit (Qiagen, Hombrechtikon, Switzerland). The single nucleotide variant rs429358 and rs7412 were genotyped using the Taqman assays C___3084793_20 and C____904973_10 respectively (Thermo Fischer Scientific, Waltham, MA, USA).

References

[10] Dayon L, Núñez Galindo A, Corthésy J, Cominetti O, Kussmann M (2014) Comprehensive and scalable highly automated MS-based proteomic workflow for clinical biomarker discovery in human plasma. *J Proteome Res* **13**, 3837-3845.

[24] Dayon L, Sanchez JC (2012) in Methods in Molecular Biology, ed. Katrin M, pp. 115-127.